นาโนแคลเซียมคาร์บอเนตจากเปลือกหอยเชอรี่และหอยนางรมเป็นสารเสริมแรง
สำหรับพอลิไวนิลคลอไรด์

นางสาวนิชธิมา รุ่งปิ่น

วิทยานิพนธ์นี้เป็นส่วนหนึ่งของการศึกษาตามหลักสูตรปริญญาวิทยาศาสตรมหาบัณฑิต
สาขาวิชาปิโตรเคมีและวิทยาศาสตร์พอลิเมอร์
คณะวิทยาศาสตร์ จุฬาลงกรณ์มหาวิทยาลัย
ปีการศึกษา 2554
ลิขสิทธิ์ของจุฬาลงกรณ์มหาวิทยาลัย

NANO CALCIUM CARBONATE FROM GOLDEN APPLE SNAIL
AND OYSTER SHELLS AS REINFORCING FILLER
FOR POLY(VINYL CHLORIDE)

Ms. Nittima Rungpin

A Thesis Submitted in Partial Fulfillment of the Requirements

for the Degree of Master of Science Program in Petrochemistry and Polymer Science

Faculty of Science

Chulalongkorn University

Academic Year 2011

Thesis Title   NANO CALCIUM CARBONATE FROM GOLDEN APPLE SNAIL AND OYSTER SHELLS AS REINFORCING FILLER FOR POLY(VINYL CHLORIDE)

By   Ms. Nittima Rungpin

Field of Study   Petrochemistry and Polymer Science

Thesis Advisor   Assistant Professor Sirilux Poompradub, Ph.D.

Thesis Co-advisor   Professor Pattarapan Prasassarakich, Ph.D.

Accepted by the Faculty of Science, Chulalongkorn University in Partial Fulfillment of the Requirements for the Master's Degree

.... Dean of the Faculty of Science

(Professor Supot Hannongbua, Dr.rer.nat.)

THESIS COMMITTEE

....Chairman

(Assistant Professor Warinthorn Chavasiri, Ph.D.)

....Thesis Advisor

(Assistant Professor Sirilux Poompradub, Ph.D.)

....Thesis Co-advisor

(Professor Pattarapan Prasassarakich, Ph.D.)

....Examiner

(Assistant Professor Varawut Tangpasuthadol, Ph.D.)

....External Examiner

(Sorapong Pavasupree, Ph.D.)

นิชธิมา รุ่งปิ่น: นาโนแคลเซียมคาร์บอเนตจากเปลือกหอยเชอรี่และหอยนางรมเป็นสารเสริม แรงสำหรับพอลิไวนิลคลอไรด์. (NANO CALCIUM CARBONATE FROM GOLDEN APPLE SNAIL AND OYSTER SHELLS AS REINFORCING FILLER FOR POLY(VINYL CHLORIDE)) อ.ที่ปรึกษาวิทยานิพนธ์หลัก: ผศ.ดร. ศิริลักษณ์ พุ่มประดับ, อ.ที่ปรึกษาวิทยานิพนธ์ร่วม: ศ.ดร. ภัทรพรรณ ประศาสน์สารกิจ, 78 หน้า

ในงานวิจัยนี้ศึกษาการใช้แคลเซียมคาร์บอเนตจากเปลือกของหอยเชอรี่และหอยนางรมมา ประยุกต์ใช้เป็นสารเสริมแรงในพอลิไวนิลคลอไรด์ทดแทนแคลเซียมคาร์บอเนตที่ใช้อยู่ในอุตสาห กรรมเพื่อลดต้นทุนการผลิตและเพิ่มมูลค่าให้แก่วัสดุเหลือใช้ โดยการสังเคราะห์แคลเซียม คาร์บอเนตอนุภาคนาโนเมตรด้วยวิธีไฮโดรเทอร์มอล ศึกษาสมบัติเชิงกล สัณฐานวิทยาและความ ร้อนของคอมพอสิตพีวีซี ที่เสริมความแข็งแรงด้วยแคลเซียมคาร์บอเนตจากเปลือกหอยและเปรียบ เทียบผลเทียบกับคอมพอสิตพีวีซีที่ผสมแคลเซียมคาร์บอเนตเกรดอุตสาหกรรม จากผลการทดลอง พบว่าภาวะที่เหมาะสมในการสังเคราะห์นาโนแคลเซียมคาร์บอเนตจากเปลือกหอยเชอรี่หรือเปลือก หอยนางรมโดยวิธีไฮโดรเทอร์มอลคือที่อุณหภูมิ 100 องศาเซลเซียส เป็นเวลา 1 ชั่วโมง ได้อนุภาค แคลเซียมคาร์บอเนตขนาด 30 ถึง 850 นาโนเมตร และ 50 ถึง 246 นาโนเมตร ตามลำดับ การศึกษา ลักษณะทางสัณฐานวิทยาของคอมพอสิตพีวีซีที่เติมแคลเซียมคาร์บอเนตจากเปลือกหอยเชอรี่หรือ เปลือกหอยนางรมหลังทำการสังเคราะห์ด้วยวิธีไฮโดรเทอร์มอล พบว่าแคลเซียมคาร์บอเนตที่ เตรียมได้สามารถยึดเกาะกับพีวีซีเมทริกซ์ การทดสอบความทนทานต่อแรงดึง เปอร์เซ็นต์การยืดตัว ณ จุดขาด และความแข็ง พบว่าคอมพอสิตพีวีซีที่เติมแคลเซียมคาร์บอเนตจากเปลือกหอยเชอรี่หรือ เปลือกหอยนางรมหลังสังเคราะห์ด้วยวิธีไฮโดรเทอร์มอลมีค่าสูงกว่าก่อนสังเคราะห์ด้วยวิธีไฮโดร เทอร์มอล สุดท้ายสมบัติเชิงกลของคอมพอสิตพีวีซีที่เติมแคลเซียมคาร์บอเนตจากเปลือกหอยเชอรี่ หรือเปลือกหอยนางรมหลังสังเคราะห์ด้วยวิธีไฮโดรเทอร์มอลมีค่าใกล้เคียงกับแคลเซียมคาร์บอเนต จากเกรดทางการค้า

สาขาวิชา.ปิโตรเคมีและวิทยาศาสตร์พอลิเมอร์.ลายมือชื่อนิสิต....นิชธิมา รุ่งปิ่น....................

ปีการศึกษา.......2554...................ลายมือชื่อ อ.ที่ปรึกษาวิทยานิพนธ์หลัก..................

ลายมือชื่อ อ.ที่ปรึกษาวิทยานิพนธ์ร่วม..................

5173414723 :   MAJOR PETROCHEMISTRY AND POLYMER SCIENCE

KEYWORDS   :   CALCIUM CARBONATE / POLY(VINYL CHLORIDE) / GOLDEN APPLE SNAIL / OYSTER SHELL

NITTIMA RUNGPIN: NANO CALCIUM CARBONATE FROM GOLDEN APPLE SNAIL AND OYSTER SHELLS AS REINFORCING FILLER FOR POLY(VINYL CHLORIDE). ADVISOR: ASST. PROF. SIRILUX POOMPRADUB, Ph.D., CO-ADVISOR: PROF. PATTARAPAN PRASASSARAKICH, Ph.D., 78 pp.

This research studied the use of calcium carbonate from golden apple snail and oyster shells as reinforcing filler for poly(vinyl chloride) (PVC), in order to replace commercial calcium carbonate ($CaCO_3$) to reduce production costs and increase waste value. $CaCO_3$ was synthesized by hydrothermal process. The mechanical, morphology and thermal properties of PVC compound reinforced by $CaCO_3$ from golden apple snail and oyster shells were investigated and compared with commercial $CaCO_3$ filled PVC. The optimum condition for producing nano-$CaCO_3$ by hydrothermal process from golden apple snail or oyster shells was to set the temperature at $100^{\circ}C$ and digested for 1 h. The particle sizes of $CaCO_3$ were within the range of 30-850 nm and 50-246 nm, respectively. The morphological study of PVC composites revealed that $CaCO_3$ particles obtained from golden apple snail shells or oyster shell after hydrothermal process had good adhesive interface with PVC matrix. The tensile strength, elongation at break, and hardness of PVC composite material by adding $CaCO_3$ from golden apple snail shells or oyster shell after hydrothermal process were higher than those before hydrothermal process. Finally, the mechanical properties of $CaCO_3$ from golden apple snail or oyster shells after hydrothermal process filled PVC composite materials were similar to those of commercial $CaCO_3$ filled ones.

Field of Study: Petrochemistry and Polymer Science   Student's Signature....................

Academic Year: ....2011...................................   Advisor's Signature..................

Co-advisor's Signature..................

ACKNOWLEDGMENTS

CONTENTS

LIST OF TABLES

LIST OF FIGURES

Figure   **Page**

Figure **Page**

CHAPTER I

INTRODUCTION

1.1 The Purpose of the Investigation

Poly(vinyl chloride) (PVC) is a traditional polymer material that is widely used in many fields, such as rigid profile, cable and many other industries. Many modification ways are developed to improve its mechanical and thermal properties [1]. Now as a development in the preparation of nanoparticles and the nano-calcium carbonate (nano-$CaCO_3$) has been a commonly used reinforcement filler for PVC because of its ability to provide an increased stiffness, toughness and dimensional stability. Additionally, the use of mineral filler is not only for improving the mechanical properties but also for reducing the cost of product. Therefore, many efforts have been devoted to improve the dispersion of nanoparticles in polymer matrix, i.e., the addition of nonionic modifier, the use of ultra high speed mixer for preparation, a high content of nanoparticles [2].

The $CaCO_3$ minerals have recently taken much of interest since the carbonate minerals are the major constituent found in aquatic invertebrate exoskeletons [3]. The special properties of $CaCO_3$ from shells are high chemical purity and non toxic when compared with commercial $CaCO_3$. In this research, the golden apple snail and oyster shells composed of $CaCO_3$ are used as reinforcement filler in PVC to replace of commercial $CaCO_3$. The natural materials not only reduce the cost of plastic and its also reduces environmental problems. In Thailand, the golden apple snail, *Pomacea canaliculata* (PC), is a large freshwater snail which can be found in river, ponds, swamps, canals and paddy fields. This kind of snail is a serious rice pest in Thailand because it damages young rice seedlings [4]. Moreover, Oyster shell, *Crassostrea commercialis* (CC), are many waste obtained from fishermen harvest fresh oysters for food and shells of oysters is removed during cooking [5]. Benefits of using natural filler include the low cost, light weight, biodegradability, added value of material and reduced waste and energy consumption.

1.2 Objectives

The objectives of this research are as follows:

1.2.1 To prepare and characterize nano-$CaCO_3$ from golden apple snail and oyster shells by hydrothermal process

1.2.2 To investigate the effect of nano-$CaCO_3$ on the thermal properties and mechanical properties of PVC composite materials

1.2.3 To compare all properties of nano-$CaCO_3$ from golden apple snail or oyster shell filled PVC composites with commercial $CaCO_3$ filled ones

1.3 Scope of the Investigation

The nano-$CaCO_3$ from the golden apple snail or oyster shell were synthesized by using hydrothermal process. The nano-$CaCO_3$/PVC composite prepared at various contents of nano-$CaCO_3$. The effect of nano-$CaCO_3$ content on the mechanical properties, morphology and thermal properties were also investigated.

The experimental procedures were carried out as follows:

1.3.1 Survey literatures and study the research works

1.3.2 Prepare the nano-$CaCO_3$ from golden apple snail or oyster shells by hydrothermal process

1.3.3 Characterize the chemical structure of prepared nano-$CaCO_3$

1.3.4 Prepare PVC composites with $CaCO_3$ obtained from golden apple snail and oyster shells before and after hydrothermal processes

1.3.5 Investigate the morphology of fracture test specimen after tensile test by scanning electron microscope (SEM)

1.3.6 Investigate the mechanical properties and thermal properties of PVC composites

1.3.7 Compare all obtained result of nano-$CaCO_3$/PVC composites with those of commercial $CaCO_3$/PVC composites

1.3.8 Summarize the results and write thesis

CHAPTER II

THEORY AND LITERATURE REVIEWS

2.1   Poly(vinyl chloride) [6]

Most PVC is commercially produced by suspension polymerization. Bulk and emulsion polymerizations are used to a much lesser extent, and solution polymerization is seldom used. Suspension polymerization of vinyl chloride is generally carried out in batch reactor as shown in Figure 2.1. A typical recipe includes 180 parts water and 100 parts vinyl chloride plus small amounts of dispersants (<1 part), monomer-soluble initiator, and chain-transfer agent (trichloroethylene). All components except monomer are charged into the reactor, which is then partially evacuated. Vinyl chloride is drawn in, sometimes by using pressurized oxygen-free nitrogen to force monomer into the reactor. The reactants are then heated in the closed system to about 50°C and the pressure rises to about 0.5 MPa. When the pressure is about 0.05 MPa, corresponding to about 90% conversion, excess monomer is vented off to be recycled. Removal of residual monomer typically involves passing the reaction mixture through a countercurrent of steam. The reaction mixture is then cooled, and the polymer separated, dried in hot air at about 100°C, sieved to remove any oversized particles, and stored. Typical number-average molecular weights for commercial PVC are in the range 30,000-80,000.

PVC or *Carvic, Darvic, Geon, Koroseal, Marvinol, Nipeon, Opalon,* and *Vygen* (trade names) has very low crystallinity but achieves strength because of the bulky polymer chains. This is apparent in the high T_g of 81°C, although T_g is not so high that processing by a variety of techniques (injection molding, extrusion, blow molding, calendering) is impaired. PVC is relatively unstable to light and heat with the evolution of hydrogen chloride, which can have deleterious effects on the properties of nearby objects (e.g., electrical components) as well as physiological effects on humans. The commercial importance of PVC would be greatly reduced were it not for the fact that this instability can be controlled by blending with
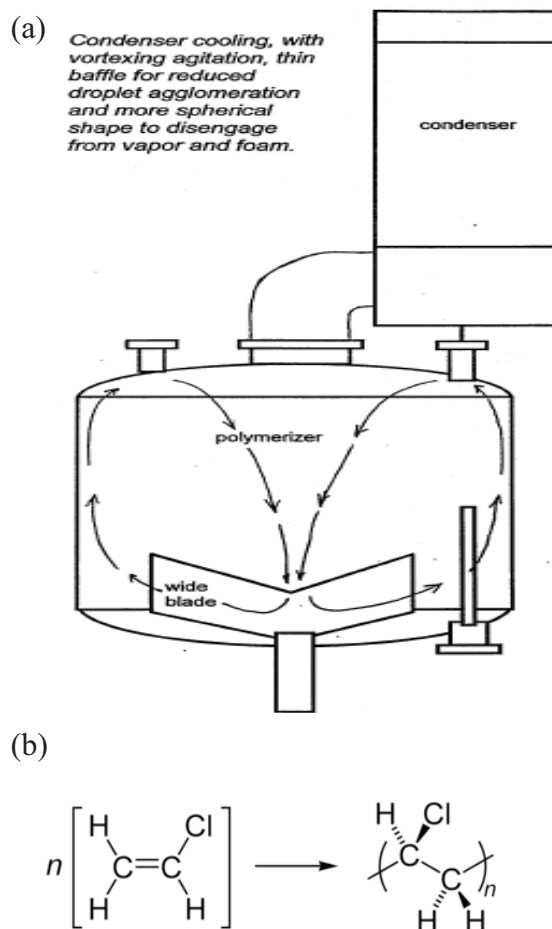
Figure 2.1 (a) Typical polymerization vessel for suspension polymerization of vinyl chloride [6].

(b) Structured of PVC [6].

appropriate additives such as metal oxides and carbonates as well as fatty acid salts. These additives stabilize PVC by slowing down the dehydrochlorination reaction and absorption of the evolved hydrogen chloride.

PVC is a very tough and rigid material with extensive applications. Its range of utilization is significantly expanded by plasticization, which convent rigid PVC to flexible PVC. Plasticization involves blending PVC with plasticizers (e.g., diisooctyl phthalate, tritely phosphate oils). The plasticizer imparts flexibility by acting effectively as an "internal lubricant" between PVC chains. Plasticization accomplishes for PVC what copolymerization and polymer blending accomplishes for polystyrene changing a rigid material into a flexible one. Blending of PVC with

rubbery polymers to improve impact strength is also practiced. More than 14 billion pounds of PVC products, about evenly divided between rigid and flexible grades, were produced in 2011 in the United States. Rigid pipe for home and other construction accounts for than 40% of the total PVC market. Vinyl siding, window frames, rain gutters, and downspouts account for another 10-15%. Packaging applications (bottles, box lids, blister packaging) account for about 8%. More than 10% of PVC is used for flooring (large sheet and tile). Other applications include wire and cable insulation for buildings, telecommunications and appliance wiring, garden hose, surgical and other protective gloves, and casted products.

2.2   Calcium Carbonates [7]

$CaCO_3$ is one of the earth's most abundant minerals, found in various forms all over the world. It is a very stable mineral, forming entire mountain ranges in addition to portions of seashores composed of coral and mollusk shell. In living organisms- from simple seashell, coral and mollusks to the most highly advanced vertebrate- structures containing $CaCO_3$ provide protection and support. Skeletal structures containing calcium phosphate and $CaCO_3$ far outlast all other body parts. $CaCO_3$ particles have three crystal morphologies, which are generally classified as rhombic calcite, needle-like aragonite and spherical vaterite. Calcite belonging to the trigonal-hexagonal-scalenohedral class is the most stable phase at room temperature under normal atmospheric conditions, while aragonite and vaterite belong to the orthorombic-dipyramidal and hexagonal-dihexagonal dipyramidal classes, respectively. Owing to the varied geologic history of $CaCO_3$ deposits, many different forms are recognized, such as limestone, marble, calcite, chalk, aragonite and dolomite. Among these, calcite and chalk as well as men-made precipitated grades are the most commercially developed forms.

2.2.1   Natural Calcium Carbonates [7]

$CaCO_3$ in the form of ground chalk, limestone or marble for use in thermoplastics should possess the characteristic properties in table 2.2.

Table 2.1   Typical properties of $CaCO_3$ from limestone [7]

Property	Value
$CaCO_3$, %	98-99.5
$MgCO_3$, %	Up to 0.5
Fe_2O_3, %	Up to 0.2
Al-silicate (colloidal), %	Up to 1.0
Loss on ignition, %	43.3-43.8
Moisture content, %	Up to 0.3
Density, g/cm^3	Up to 2.7
Mohs hardness	3
Degree of whiteness, %	85-95
pH	9.0-9.5
Oil absorption, g/100 g powder	9-21
DOP number, g/100 g powder	9-33
Specific surface, m^2/g	1-15

Table 2.2 shows the typical properties of $CaCO_3$ from limestone. Limestone was entirely composed of $CaCO_3$ 99%, low specific surface and high degree of whiteness. There is an unfortunate tendency to judge carbonate fillers solely on the basis of cost. Geological origin, chemical purity, i.e. amount and kind of impurities, treatment method and subsequent surface finishing are, however, of utmost importance, particularly as regards use in the plastics industry.

Leading companies are nowadays able to supply custom-made fillers for various fields of application which eliminate undesirable side effects on processing machinery (wear) and on the mechanical properties of the finished articles. An additional factor is that a lipophilic character can be imparted to calcium carbonate by a suitable surface treatment (coating). This appreciably facilitate its use in thermoplastics.

2.2.2   Synthetic, Precipitated Calcium Carbonates [7]

These fillers also known as CCP ($CaCO_3$ praecipitatum) possess the characteristic properties in table 2.3.

Table 2.2   Typical properties of precipitated $CaCO_3$ [7]

Property	Value
$CaCO_3$, %	98-99.5
Degree of whiteness, %	85-95
Oil absorption, g/100 g powder	9-21
Specific surface, m^2/g	1-15

The special properties of precipitated, surface-treated $CaCO_3$ result from their small particle size, their high degree of purity, and their aragonite structure. As a consequence of the surface treatment in question, good dispersibility in the polymer matrix is thereby achieved.

Like the ground carbonates, precipitated $CaCO_3$ are frequently used in plastics such as PVC and influence their properties as follows :

- Increased impact strength (especially in unplastized PVC),
- High surface gloss of finished products, good elongation at break, tear propagation resistance and tensile strength,
- Reduced plate out,
- Good weathering stability,
- Strong influence on the rheology of plastisols.

Compared with natural, ground $CaCO_3$, the synthetic, precipitate $CaCO_3$ fillers do, however, have the following disadvantages :

- More expensive,
- Due to the larger specific surface, the shearing forces during processing are appreciably higher,
- Greater absorptive effects on plasticizers, stabilizers, lubricants etc.

2.3   Source of Natural Calcium Carbonate [8,9]

$CaCO_3$ is abundant in nature. The most commonly used source of $CaCO_3$ for the commercially developed forms are golden apple snail and oyster shells.

2.3.1   Golden apple snail shell [8]

The golden apple snail, *Pomacea canaliculata* (PC) have been called as pond snail or river snails which are found widespread in shallow freshwater and light saline water in Thailand such as ponds or brooks, coastal areas, gulfs and basins where the sediment is mud or sandy mud. However, golden apple snail is native to South America. It was introduced from Argentina into Thailand in the 1982s for commercial production. From there, it was later distributed to most Asian countries as a protein supplement in the diet and as income earner for the rural poor. However, the introductions were done in haste with no prior studies on economic benefits and ecological impacts in the new environment. When market demand for the snail was poor, many snail-farming projects were abandoned and in many instances the snails escaped and subsequently became a pest of crops. Rice crops were particularly affected. When the golden apple snail began to attack the rice crop, information on its ecology, biology and control measures were lacking, so pesticides were selected rather arbitrarily and were applied inappropriately causing environmental pollution and hazard to public health. Farmers suffered a range of health problems. The golden apple snail is now a major rice pest in Asia. Several control techniques are now available; these include biological, cultural and chemical controls. However, a non-chemical control approach is preferable, as excessive applications of pesticides are hazardous to the environment.

Since the golden apple snail shell mainly consists of aragonite and a fraction of calcite, it may be used like $CaCO_3$. Therefore, there are very experimental studies on the use of naturally renewable materials of the golden apple snail shell as a filler to replace the commercial $CaCO_3$, which is usually used in many industries.

2.3.2   Oyster shell [9]

In Thailand, people consume a fair amount of shellfish including oysters shell *crassostrea commercialis*, hard clams and freshwater clams. Among them, oysters are the most consumed, and around 168,500 tons of waste oyster shell was produced in 2007. Due to increasing seafood consumption, a large amount of waste shells are being generated and discarded. Improper disposal could cause environmental pollution and sanitary problems. Recycle of these fishery residues can be a good alternative to disposal, and some researches have been done in this area. For instance, oyster shell was used as an adsorbent to treat SO_2/NO_x in polluted air and to form precipitates with phosphate to alleviate eutrophication problems. Additionally, crab shell or crab-generated chitosan were used as adsorbents for metal ions removal. However, these methods of recycling shells may generate plenty of spent adsorbents and introduce secondary pollution. To overcome this, development of a more effective reuse of waste shells is warranted. The crystal structure of $CaCO_3$ from oyster shell are composed of calcite form as opposed to aragonite in nacre. The main composition of oyster shell was $CaCO_3$ which have attracted attention because of their low cost.

2.4   Manufacturing Processes [10]

2.4.1   Purified Fine Ground Calcium Carbonates [10]

This type of $CaCO_3$ has the widest usage in plastics because it is purified by chemical or physical removal of iron and silica minimize the degradation of plastics, and is ground fine enough to provide good physical properties in highly filled plastic compound. Production is straightforward, using equipment and procedures described in detail in Perry's Chemical Engineers' handbook and Riegel's Industrial Chemistry. The stone is usually quarried, but in some cases underground mining is used. The crude rock is "crushed" in a jaw of roll crusher to pass through a 3-inch screen, and further particle size reduction can occur in pot crushers, rotary hammer mills, of similar mills to reach 100 mesh in size.

Chemical flotation or mineral dressing to remove impurities can be done at this size or at any of several later stages in the size reduction process. Particle size reduction can continue using dry or water grinding techniques, utilizing grinding media. Once the general particle size range is reached, classification techniques may function to produce select particle size distributions. Water-ground products are shipped as slurry of dried and micronized. This type of process will generally be used for products having a median particle diameter of 0.6 to 10 μm as measured by ASTM D3360-80. (Micrometer is the metric term for one millionth of a meter, symbol μm. the earlier term, micron, is still in common use.)

2.4.2   Dry Process Coarse Calcium Carbonates [10]

For some applications, such as vinyl foam, carpet backing, and inexpensive dark floor tiles, fairly coarse unpurified $CaCO_3$ is used. Processing is simple followed by air separation; that is removal of oversize particles by a counteraction "whizzer" or multivane "deflector". Products in this category generally have a median particle diameter greater than 12 μm.

2.4.3   Solvay Process [10]

Ernest Solvay, a Belgian, in 1864, successfully manufactured Na_2CO_3 by an ammonia process shown in eq. 2.1.

$$NH_3 + H_2O + CO_2 + NaCl \leftrightarrows NaHCO_3 + NH_4Cl \qquad (2.1)$$

$$2NaHCO_3 + heat \rightarrow Na_2CO_3 + H_2O + CO_2$$
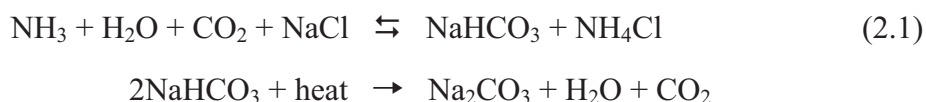
$CaCO_3$ is used in this process shown in eq. 2.2.

$$CaCO_3 + 2HCl \rightarrow CaCl_2 + CO_2 + H_2O \qquad (2.2)$$

$$CaCl_2 + Na_2CO_3 \rightarrow CaCO_3 + 2NaCl$$
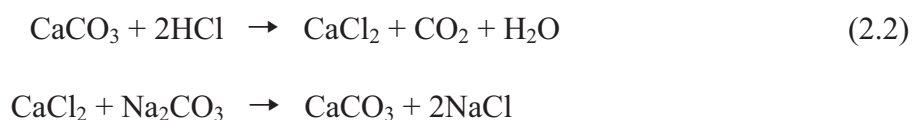
Naturally occurring $CaCO_3$ is a starting material and in this process precipitated $CaCO_3$ is a by-product. Production of the byproduct is limited by amount of main product produced. Precipitated $CaCO_3$ is washed to remove soluble salts, then dried and micropulverized. The particle size is controlled by conditions of precipitation: temperature, concentration, rate and order of addition of ingredients, and amount of agitation. Particle sizes are fairly uniform and can be varied from about 0.03-0.05 μm up to about 8-10 μm. Precipitated $CaCO_3$ is used in specialized applications where purity and excellent whiteness justify their higher cost.

2.4.4   Lime Soda Process [10]

Since 1940, more NaOH has been produced electrolytically than by the "lime-soda" process described in this section. Therefore, the production of precipitated $CaCO_3$ by this process is necessarily limited. In this lime-soda process, $CaCO_3$ is heated to form CaO and reacted with water to form calcium hydroxide $Ca(OH)_2$. the $Ca(OH)_2$ is then reacted with sodium carbonate to form calcium carbonate and sodium hydroxide, as shown in eq. 2.3.

$$Na_2CO_3 + Ca(OH)_2 \leftrightarrows 2NaOH + CaCO_3 \qquad\qquad (2.3)$$

The $CaCO_3$ settles out, is removed and washed to remove NaOH. Fine particle size $CaCO_3$ is available. Finely ground purified $CaCO_3$ is replacing the by-product material for many used; where precipitated $CaCO_3$ is still required, it is manufactured by a more direct process described in the following section.

2.4.5   Precipitated Calcium Carbonates by Recarbonation [10]

This process consists of heating $CaCO_3$ to form CO_2 + CaO that is reacted with water to form $Ca(OH)_2$. The CO_2 is saved and recombined with the $Ca(OH)_2$ as shown in eq. 2.4.

$$CaCO_3 \xrightarrow{heat} CO_2 + CaO \xrightarrow{H_2O} Ca(OH)_2 \xrightarrow{CO_2} CaCO_3 \qquad\qquad (2.4)$$
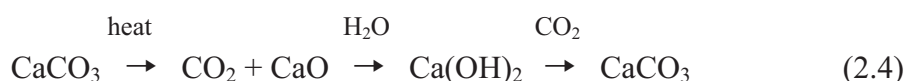
The product is aragonite, with higher sp.gr. than calcite. Median particle sizes are between 0.2 and 2.0 µm, and particle size distribution is wider than the previous two precipitate materials.

Advantages of precipitated $CaCO_3$: High purity grades for U.S.P, FDA and food contract uses; very fine particle sizes for high viscosity non-sag plastisols and polyesters.

Disadvantages: higher cost, higher energy to manufacture, ionic and water content must be taken into consideration, fineness causes excessive viscosity in some polyesters.

2.5   Technique for Synthesis of Calcium Carbonate Nanoparticles [11-13]

$CaCO_3$ nanoparticles can be prepared on a large scale at low by simple solution-based methods such as chemical precipitation, sol-gel synthesis and solvothermal/hydrothermal reaction.

2.5.1   Chemical Precipitation [11]

The precipitation method is studied in this work because it is relatively simple and it has already been demonstrated that it is possible to fabricate superfine precipitated calcium carbonate particles using this method. There are two precipitation methods in the literature with the only difference being the chemicals used. The first method is mixing calcium hydroxide ($Ca(OH)_2$) and water into a slurry and carbonating the solution with CO_2 bubbles to form $CaCO_3$. The alternative chemical combination used is a mixture of sodium carbonate (Na_2CO_3) and calcium chloride ($CaCl_2$) which would also form $CaCO_3$.

The precipitation process usually produces precipitated $CaCO_3$ particles that are of spindle shape and having a particle size of more than 2 µm, however, much finer particles of different morphologies can be produced in the process as to be discussed below. It is therefore desirable to understand how the operating parameters affect the particle size of the particles produced, so that the carbonation process can be optimized to fabricate particles of desired size, particularly superfine size.

2.5.2 Sol-Gel Synthesis [12]

The sol-gel technology emerged within the last two decades and quickly became one of the most important and promising new material fabrication methods for nanoscale materials and nanotechnology. It enables researcher to design and fabricate a wide variety of different material with unique chemical and physical properties. The sol-gel materials are based on silica, alumina, titania and other compounds. The sol-gel technology allows to fabricate: monolithic and porous glasses, fibers, powders, thin films, nanocrystallites photonic crystals. A broad spectrum of difference sol-gel derived materials opens a variety of new applications in a broad range of fileds: opto-electron (optical sensors, lasers, filters, photonic crystals), new chemicals for agriculture, pharmacy (controlled drug delivery systems).

Sol-gel technology is concerned with the production of metal oxides. The sol-gel technique basically creates a three-dimensional network of inorganic mater, known as gel, from a colloidal or molecular solution of the precursor (sol), by low temperature polymerization. The wet gel is dried to remove water. The porous gel is then converted into glass or ceramic. The most commonly used starting materials are metals alkoxides. These are either used alone or mixed with other species to from complexes, which then can act as precursors for the end mixed metal oxides.
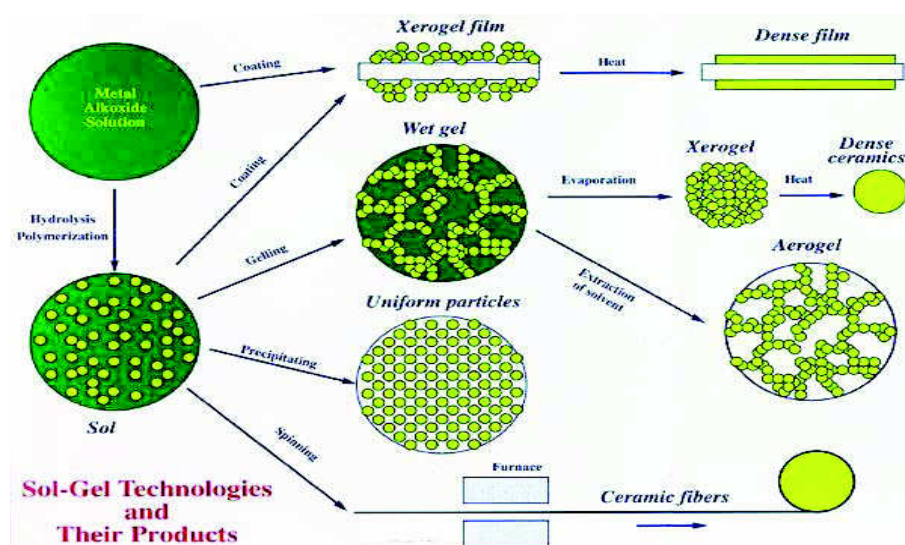
Figure 2.2 An overview of the sol-gel process [12].

Sol-gel processing is a versatile technique for the preparation of inorganic and hydrid organic-inorganic material. Its mild conditions and capability for controlling composition, multiple levels of structure, porosity, mechanical properties, chemical functionality, optical properties and ultimate form make sol-gel processing a powerful tool. Many questions remain unanswered regarding aspects of reaction mechanisms, molecular level control over properties, physics of gelation and postgelation processing and creation of nanostructures.

2.5.3 Hydrothermal Synthesis [13]

Hydrothermal synthesis is a method that is widely used for the production of (ultra) small powder and particles especially in the ceramics industry. Recent research has showed the possibility of using this method for the systhesis of ID (nanotube, nanowrods, nanowires) metal oxides.

Hydrothermal techniques are a particular case of solvothermal process. The hydrothermal method involves the heating of solid and liquid reagents with a suitable solvent (usually water) in a sealed vessel at temperature of up to $250^{o}C$. Although elevated temperatures are used and pressure is generated in the sealed container, the conditions are much less severe than the traditional ceramic methods of solid-state chemistry. These mild, solvent-mediated, reaction conditions have allowed access too many novel materials with important applications.

In nanotechnology, the hydrothermal technique has an edge over other materials processing techniques, since it is an ideal one for the processing of designer particulates. The term designer particulates refers to particles with high purity, high crystallinity, high quality, monodispersed and with controlled physical and chemical characteristics. Today such particles are in great demand in the industry. Figure 2.3 shows the major differences in the products obtained by ball milling or sintering or firing and by the hydrothermal method. In this respect hydrothermal technology has witnessed a seminal progress in the last decade in processing a great variety of nanomaterials ranging from microelectronics to micro-ceramics and composites.
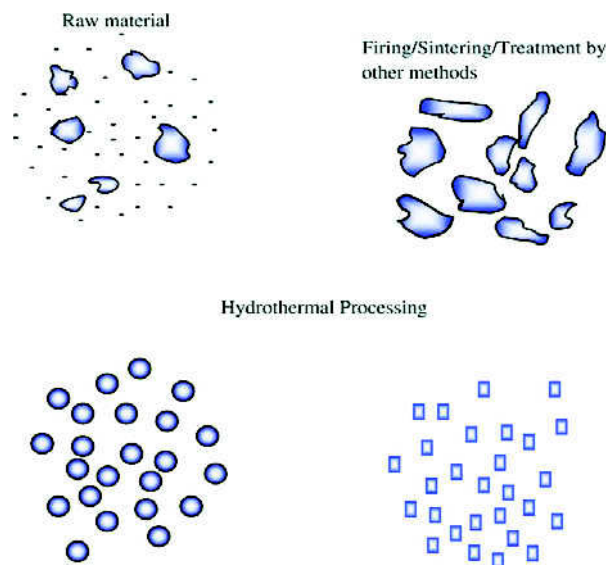
Figure 2.3 Difference in particle processing by hydrothermal and
conventional techniques [13].

In this work, nano-$CaCO_3$ was prepared by using hydrothermal process.
Benefits of using hydrothermal process are use of larger volume equipment, lower
temperature operations in the presence of the solvent and energy saving.

2.6   Use of Natural Calcium Carbonate in Rigid PVC [14]

As with PVC, natural $CaCO_3$ grades are the main fillers used in rigid PVC,
although only the type with very small particle size and surface-treated forms are
employed. The latest technological developments have shown that a considerable
increase in the filler content can be achieved if the impact resistance is raised by the
addition of suitable impact modifiers. Chlorinated polyethylene and other products
improving impact strength such as polyacrylates or polyvinyl acetate permit a filler
content of over 30 part by wt, chalk to 100 parts by wt. PVC.

The use of coated $CaCO_3$ results in increased stiffness, lower shrinkage and
reduced plate out; notched impact strength is increased and aging resistance and
temperature of deflection under load are improved in comparison with unfilled
PVC-U. Extrudability is better and the cost per unit volume lowered.

2.7   Use of Precipitated Calcium Carbonate in Rigid PVC [14]

These are chiefly used in rigid PVC. However, the small particle size of this class of fillers leads to a strong increase in torque in the processing machines, with the result that the permissible filler volumes are far lower than with ground $CaCO_3$ grades. Precipitated carbonates improve surface, shade, degree of whiteness, surface gloss and plate out. The modulus of elasticity rises, but the other mechanical properties are not greatly influenced.

2.8   Literature Reviews

Zhaodong *et al.* [15] studied the abnormal structure conversion of $CaCO_3$ from calcite to aragonite with a mixture of polyacrylamide (PAM) and cetyltrimethyl-ammonium (CTAB) as additive by a hydrothermal method. A novel morphology of aragonite, magnified cubic shape. Rod-like aragonite crystals were synthesized without any additive at 90 and 120^oC. The mixture of calcite and vaterite was obtained with PAM as additive at 90 and 120^oC. The results indicate the temperature and the interaction between the mixed template and the $CaCO_3$ important roles in the process of structure transformation.

Takuya *et al.* [16] studied the synthesis of calcite ($CaCO_3$) nanoparticles by mechanochemical reaction and subsequent heat treatment was investigated. A solid-state displacement reaction of $CaCl_2$ and Na_2CO_3 to from $CaCO_3$ and NaCl was induced during mechanical milling of a $CaCl_2$ and Na_2CO_3 powder mixture. Heat treatment of the as-milled powder at 350^oC completed the reaction, forming crystalline $CaCO_3$ nanoparticles separated from each other in a dry-salt matrix. The mean particle size was controlled by changing the volume fraction of $CaCO_3$ in the matrix. 20% volume fraction yielded nanoparticles of 140 nm in size, whereas 10% volume fraction led to 80 nm size nanoparticles.

Hernandez *et al.* [17] studied the hydrothermal carbonation of calcium hydroxide ($Ca(OH_2)$) at high pressure of CO_2 (55 bar) and high temperature (30 and 90^oC) was preparation particles size of calcite. While nanoparticles are obtained at 55 bar and 30^oC average particle size less than 200 nm, the sub-micrometric average

particle size of 0.22 to 1 μm assuming calcite form well defined crystals are obtained at 90 bar and 90°C. The XRD and BET specific surface areas decreases from 5 to 3 when changing the initial thermodynamic conditions from 50 bar and 30°C to 90 bar and 90°C. This demonstrates that better crystallized samples are obtained when raising the pressure conditions and temperature, and a higher degree of aggregation of the crystallites in the 50 bar and 30°C samples.

Udomkan *et al.* [18] studied the thermal decomposition process of *Pomacea canaliculata* Lamarck (PCL) samples. A set of 4 samples each was then separately annealed for 2 h in air atmosphere at 300°C, 400°C, 450°C and 500°C, respectively. The PCL shell mainly consists of aragonite and a fraction of calcite. When the PCL powder samples were annealed at a temperature higher than 450°C, it resulted was change the phase transition from aragonite to calcite.

Zeng *et al.* [19] studied the mechanical and rheological properties of the PVC composites. PVC composites filled with $CaCO_3$ particles with different diameter (about 40, 80, 500, 25000 nm) were prepared by using a single-screw extruder. The results showed that while the diameter of $CaCO_3$ nanoparticles was smaller, the mechanical properties of composites were higher than microparticles. By adding $CaCO_3$ 40-nm into the PVC matrix, the single-notched impact strength of the nanocomposite higher than PVC blend filled with micro-$CaCO_3$. The tensile and flexural properties of nanocomposites were also prior to those of the composites with 500-nm and 25-μm $CaCO_3$ particles. The $CaCO_3$ particles could make the rheological property of PVC composites worse. When the mass ratio of nano-$CaCO_3$ and micro-$CaCO_3$ was 2.5 and 9, the profile could obtain good mechanical properties of PVC door and window profile in industry.

Linna Hu et al. [20] studied the new technique in an environmentally and reduce energy consumption. Linseed oil which is vegetable grease as modification agent, therefore, friendly process. Active $CaCO_3$ nanoparticles were directly prepared via carbonation of $Ca(OH)_2$ slurry in the presence of linseed oil at 20°C. When the weight ration of linseed oil to $CaCO_3$ nanoparticles was 3%, the active ratio of the product was 99.07%. The mechanical properties of PVC composite materials were significantly improved. When adding the active $CaCO_3$ nanopartices into PVC (the weight ratio of $CaCO_3$ nanoparticles to PVC about 10:100).

CHAPTER III

EXPERIMENTAL

3.1 Materials

The chemicals which are used in this study are shown in Table 3.1.

Table 3.1 Chemicals that are used for study.

Chemicals	Function	Commercial Name	supplier
Oyster shell	Natural calcium carbonate	Oyster	Rayong Province
Golden apple snail shell	Natural calcium carbonate	Golden apple	Chiangmai Province
Nano calcium carbonate	Reference	NPCC B800	Nano materials Technology Pte. Ltd.
Micro calcium carbonate	Reference	OMYA-2	Surint Omya Chemical
Sodium carbonate	Synthesis Calcium carbonate	Sodium carbonate AR grade	Merck Co.,Ltd.
Hydrochloric acid	Solvent	Hydrochloric acid 35% AR grade	Merck Co.,Ltd.
Deminerized water	Solvent/ Cleaning solvent	Deminerized water	Riken (Thailand) Ltd.
PVC resin	Base polymer	SM-660	Riken (Thailand) Ltd.
Dioctyl phthalate	Plasticizer	Dioctyl phthalate (DOP)	Riken (Thailand) Ltd.
Polyethylene-based lubricant	lubricant	HIWAX220MP	Riken (Thailand) Ltd.
Methyl methacrylate styrene	Impact modified	B22 (MBS)	Riken (Thailand) Ltd.
Ca-Zn stabilizer	Stabilizer	RX-207	Riken (Thailand) Ltd.

3.2 Instruments

The instruments which are used in this study are shown in Table 3.2.

Table 3.2 Instruments that are used for study.

Instruments	Manufacturer
X-ray diffraction	Bruker AXS.
X-ray fluorescence	Philips
Fourier transform infrared spectroscopy	Perkin Elmer Inc.
Scanning electron microscope	Jeol Ltd.
Auto fine coater	Jeol Ltd.
Transmission Electron Microscopy	Jeol Ltd.
Hydraulic hot press	Labtech Engineering Company Ltd.
Two roll mill	Labtech Engineering Company Ltd.
TGA/DSC 1	Mettler-Toledo International Inc.
Universal Testing Machine	LLOYD Instruments LR 5K Plus
Hardness Testing Machine	Zwick
Impact Testing Machine	SWICK/Materialpruefung
Oxygen Analyser	Toyoseiko
pH meter	TOA Electronic Ltd.
Oven	Binder
Analytical and Precision Balances	Sartorius
Thermometer	Mettler-Toledo International Inc.

3.3   Material Preparation

The exoskeletons of freshwater snail, golden apple snail shells and oyster shells living in habitat in Thailand were used as raw materials. The materials were washed in water for several times and dried under the sun. The cleaned materials were ground into fine powder then sieved with a 74 µm-mesh sieve. The outline for preparation of golden apple snail and oyster shells are shown in Figure 3.1.

(a)   **(b)**

Golden apple snail shell   Oyster shell

Golden apple snail shell particles   Oyster shell particles
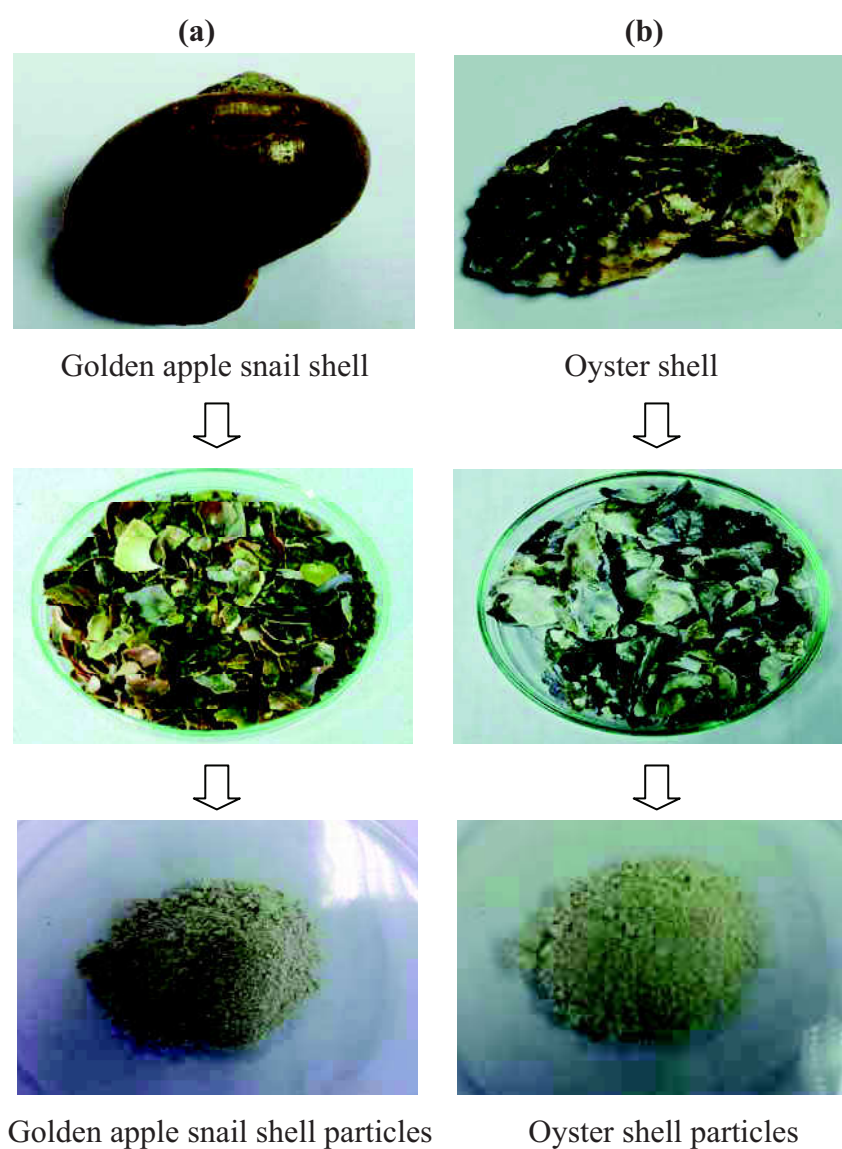
Figure 3.1 Outline for preparation of (a) golden apple snail shells particles
(b) oyster shells particles.

3.4 Synthesis Nano-CaCO$_3$ by Hydrothermal Process

In a typical hydrothermal synthesis, 50 g of golden apple snail shells and oyster shells were mixed in 500 ml of 2 M HCl. The solution was stirred at room temperature for 30 min to from CaCl$_2$ slurry. Subsequently, 500 ml of 1, 2 and 3 M Na$_2$CO$_3$ solution were added into the solution to generate CaCO$_3$. The obtained solution was then put into a teflon-lined stainless steel autoclave and heated at various temperatures (90, 100, 110, 120 and 130°C) for 1, 10 and 20 h with stirring condition. After cooled to room temperature, the obtained product was washed with distilled water and dried at 100°C for 12 h. The teflon-lined stainless steel autoclave is shown in Figure 3.2

Figure 3.2 Teflon-lined stainless steel autoclave

3.5   Characterization of CaCO$_3$ Before and After Hydrothermal Process

The crystalline structure of CaCO$_3$ particles were evaluated by XRD (Philips Model PW2400, Netherlands). The diffraction angle (2Θ) was varied from 5° to 80° using the scanning speed of 2°/min. Chemical analysis was determined by XRF (Bruker model D8-Discover, Germany) operated at 100 kV excitation voltage and a primary current of 6 mA. The K$_\alpha$ line was used at 23.17 KeV and measurement time was 1800 seconds live time per sample. The FT-IR spectra were performed on Perkin Elmer FT-IR spectrometer (model PE 2000, United states) in the wave number region 400-4000 cm^{-1}. All FT-IR measurements were carried out at room temperature using the KBr pellet technique. The microstructure of the prepared materials was analyzed by SEM (JEOL model JSM-6400, Japan) operated at 20 kV and TEM (JEOL model JEM-2010, Japan) operated at 200 kV.

The thermal properties of the CaCO$_3$ investigated by using thermogravimetric analyzer (Mettler-Toledo, TGA/DSC 1, LF, United states). The sample was place in aluminium oxide crucible. The temperature was raised under air atmosphere from room temperature to 1000 °C at continuous heating rate of 10 °C/min. The air flow rate was 50 ml/min. The initial composition and the temperature at maximum loss were evaluated.

3.6   Composites Preparation

The PVC composites were prepared according to the formulation in Table 3.3. All components were mixed on a two-roll mill at 150°C for 4 min and rolled out to be about 2 mm thick sheets. The filler contents were varied as 0, 5, 10, 15 and 20 phr. The compoundings were molded into 1 mm thick sheets by compression molding at 175°C for 2 min, and followed by cooling to room temperature.

Table 3.3   Composition of PVC composites

Material	Quantity (phr)[1]
PVC resin	100
Dioctyl phthalate (DOP)	4
HIWAX220MP	1
B22 (MBS)	5
RX-207	4
Crushed golden apple snail[2]	0, 5, 10, 15, 20
Crushed oyster shell[3]	0, 5, 10, 15, 20
NPCC B800 commercial $CaCO_3$[4] (non surface modification)	0, 5, 10, 15, 20
OMYA-2 commercial $CaCO_3$[5] (non surface modification)	0, 5, 10, 15, 20

[1]Parts per hundred parts of resin.

[2]The particle size of 0.65 µm.

[3]The particle size of 0.97 µm.

[4]The particle size of 80 nm.

[5]The particle size of 2.88 µm.

3.7   Mechanical Properties

3.7.1   Tensile Properties

The tensile properties of composite materials were determined according to ASTM D 638. The test was carried out on a universal testing machine (LLOYD Instruments LR 5K Plus, United states) with a crosshead speed of 20 mm/min. The elongation of specimens was determined by the extensometer. The report value was the average of five specimens for each test. An average of five specimens was reported as a representative value. The results of tensile properties were determined as an average. The dumbell specimen are shown in Figure 3.3.
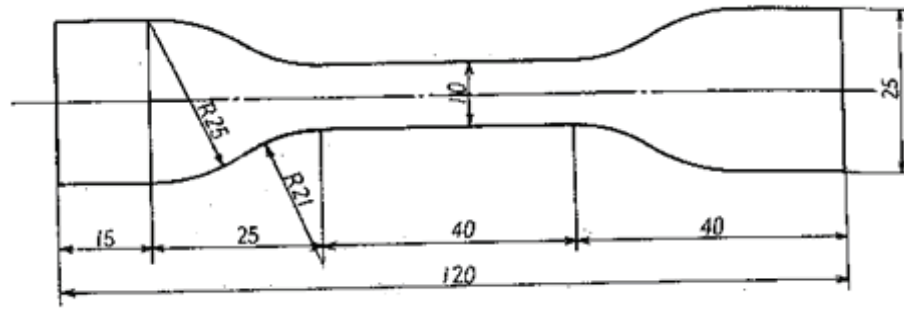
Figure 3.3 Tensile test specimen (unit: mm.) [21].

3.7.2 Izod Impact Strength

The Izod impact strength of test specimen was measured according to ASTM D 256. Izod impact strength was measured by Izod impact machine (SWICK, Materialpruefung, Germany) at the test condition of 23 ± 2°C and 50 ± 5 %RH. An average of five specimens was reported as a representative value. The bar specimen with nothced are shown in Figure 3.4.
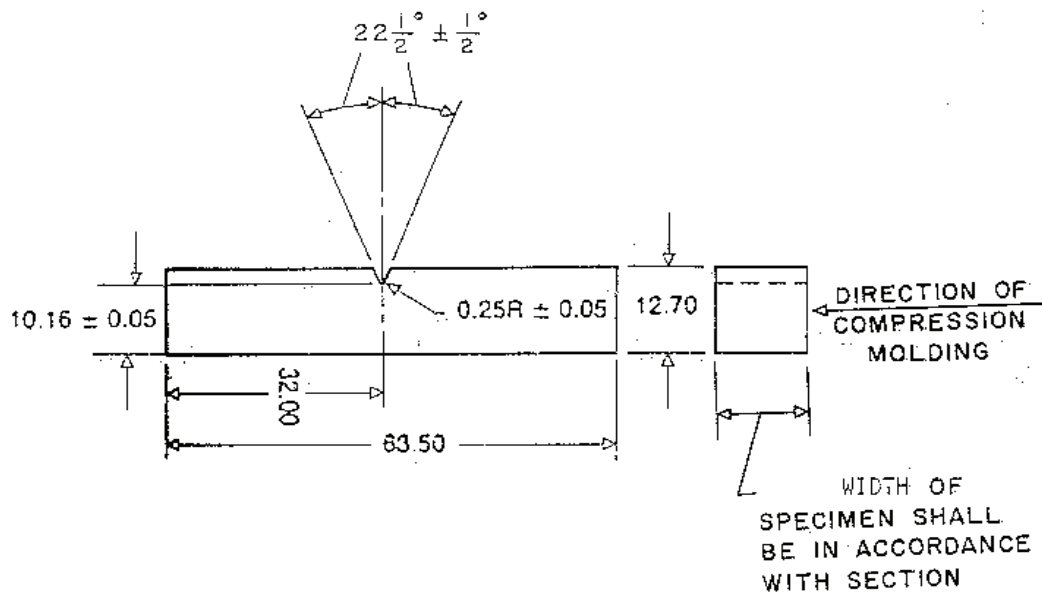
Figure 3.4 Izod impact strength test specimen (unit: mm.) [22].

3.7.3   Hardness properties

The hardness for each sample was determined according to ASTM D 2240. The test was carried out by a DURO meter (Zwick, shore A, United states). The report value was the average of five specimens for each test.

3.8   Morphological Study

The morphology of $CaCO_3$ before and after hydrothermal process and composite materials were investigated by using a SEM (JEOL model JSM-6400, Japan) at 20 kV. The synthesis $CaCO_3$ was dispersed in ethanol solution, while the sample of composite materials were fractured under cryogenic condition by using liquid nitrogen. The specimens were then mounted on a SEM stubs using a double-side tape and the fracture surface of specimens was sputtered with a thin gold layer.

3.9   Thermal stability

The PVC composite materials were compression moulded at $180^{o}C$ into 1 mm thick sheets and cut into 0.3x3.8cm strips. These strips were placed in a oven (Binder Model FD53, United states) at $190\pm1^{o}C$. Strips were removed every 30 min and subjected to visual examination.

3.10 Limiting Oxygen Index

Limiting Oxygen Index (LOI) is the minimum concentration of oxygen, determined in a flowing mixture of oxygen and nitrogen that will just support flaming combustion of the material. The oxygen concentration of the mixture used in each successive test is increased or reduced by a small amount until the required concentration is reached. All the tests were carried out according to the ASTM D 2863, which describes the procedure for testing plastic samples cut from rigid sheet. The instrument used was a Toyoseiko, Japan provided with an Oxygen Analyser. The report value was the average of five specimens for each test.

CHAPTER IV

RESULTS AND DISCUSSIONS

4.1   Characterization of Golden Apple Snail Shells and Oyster Shells Particles

4.1.1   X-Ray Fluorescence, XRF

The chemical composition of golden apple snail shell and oyster shell particles which were analysed by XRF as shown in Table 4.1. Golden apple snail shells was entirely composed of $CaCO_3$ about 99% and other oxide compounds about 1%, while that of oyster shells was entirely composed of $CaCO_3$ about 97% and other oxide compounds about 3%, respectively.

Table 4.1 Chemical composition of golden apple snail shells and oyster shells by
        XRF.

Sample	Chemical composition (%)										
	$CaCO_3$	Na_2O	Al_2O_3	SiO_2	P_2O_5	SO_3	Cl	K_2O	MaO_2	Fe_2O_3	SrO
Golden apple snail	99.302	0.307	0.033	0.126	0.021	0.044	0.015	0.022	0.069	0.050	0.011
Oyster shell	96.715	0.829	0.313	0.964	0.143	0.46	0.376	0.052	-	0.122	0.027

4.1.2   X-Ray Diffraction, XRD

Figure 4.1 shows the XRD patterns of golden apple snail shells and oyster shells, respectively. Their XRD patterns showed different crystalline peaks. Crystal of golden apple snail shells was found an aragonite form of $CaCO_3$ with orthorhombic shape, while that of oyster shells was a calcite form, calcite form, which is the hexagonal rhombohedral shape [23].
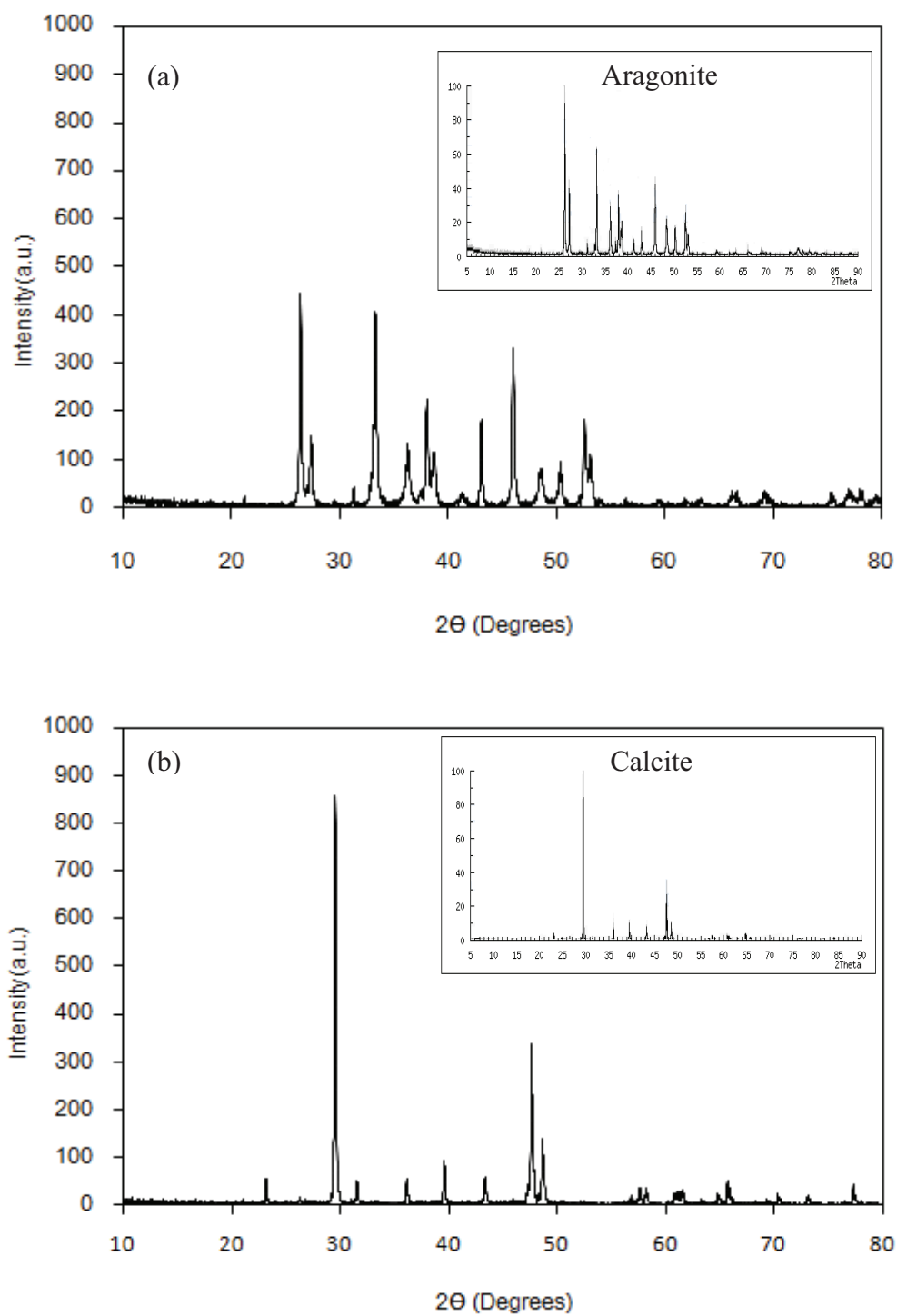
Figure 4.1 XRD patterns of (a) golden apple snail shell particles and
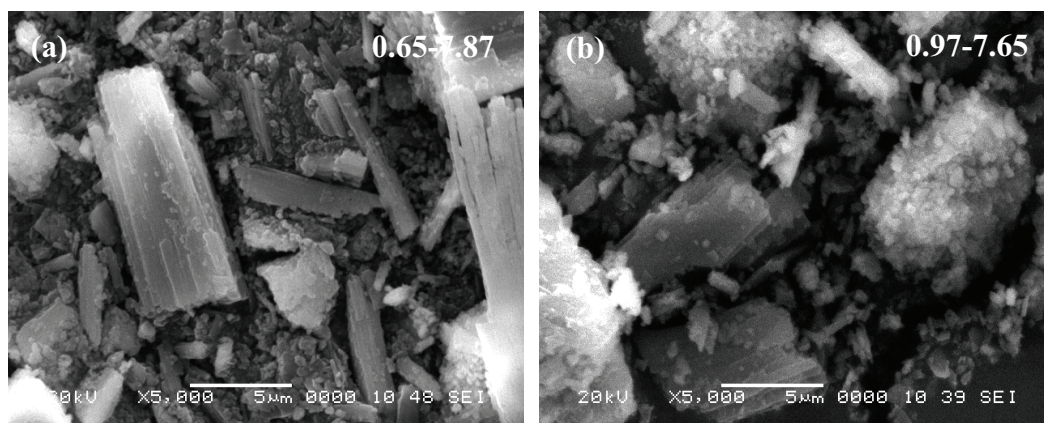(b) oyster shell particles.

Figure 4.2 SEM images of (a) golden apple snail shell particles and
(b) oyster shell particles.

4.1.3 Scanning Electron Microscopy, SEM

The crystalline morphologies of golden apple snail shells and oyster shells were observed by a SEM and the results are shown in Figure 4.2. In Figure 4.2(a) the $CaCO_3$ from of golden apple snail shell particles is aragonite in the rod shape with diameter of 0.65-7.87 μm, while that of $CaCO_3$ from oyster shell particles is cubic shape with diameter of 0.97-7.65 μm. Generally, the cubic shape is the typical morphology of calcite (Figure 4.2(b)).

4.1.4 Fourier Transform Infrared Spectroscopy, FT-IR

Figure 4.3 shows FT-IR spectra of golden apple snail shells and oyster shells. Figure 4.3(a) showed the vibrational bands at about 1083.12 and 861.86 cm^{-1} could be assigned to the characteristic symmetric carbonate stretching (v_1 mode) and carbonate out-off-plane bending (v_2 mode) vibration of aragonite. The pair of bands at about 699.95 and 713.01 cm^{-1} could be attributed to the in-plane bending modes (v_2 mode) of aragonite. In contrast, in Figure 4.3(b), the bands at 877.33 and 712.63 cm^{-1} can be attributed to the out-off-plane bending (v_2 mode) and carbonate in-plane-bending (v_4 mode) of calcite. In addition, a weak peak at 1477.89 and 1421.55 cm^{-1} in Figures 4.3(a) and (b), respectively, could be assigned to the stretching vibration of

C=O band in carboxylate of $CaCO_3$. According to FT-IR spectra, it is clearly seen that the peaks at 1083.12 and 699.95 cm^{-1} showed the characteristic peak of aragonite form [23].
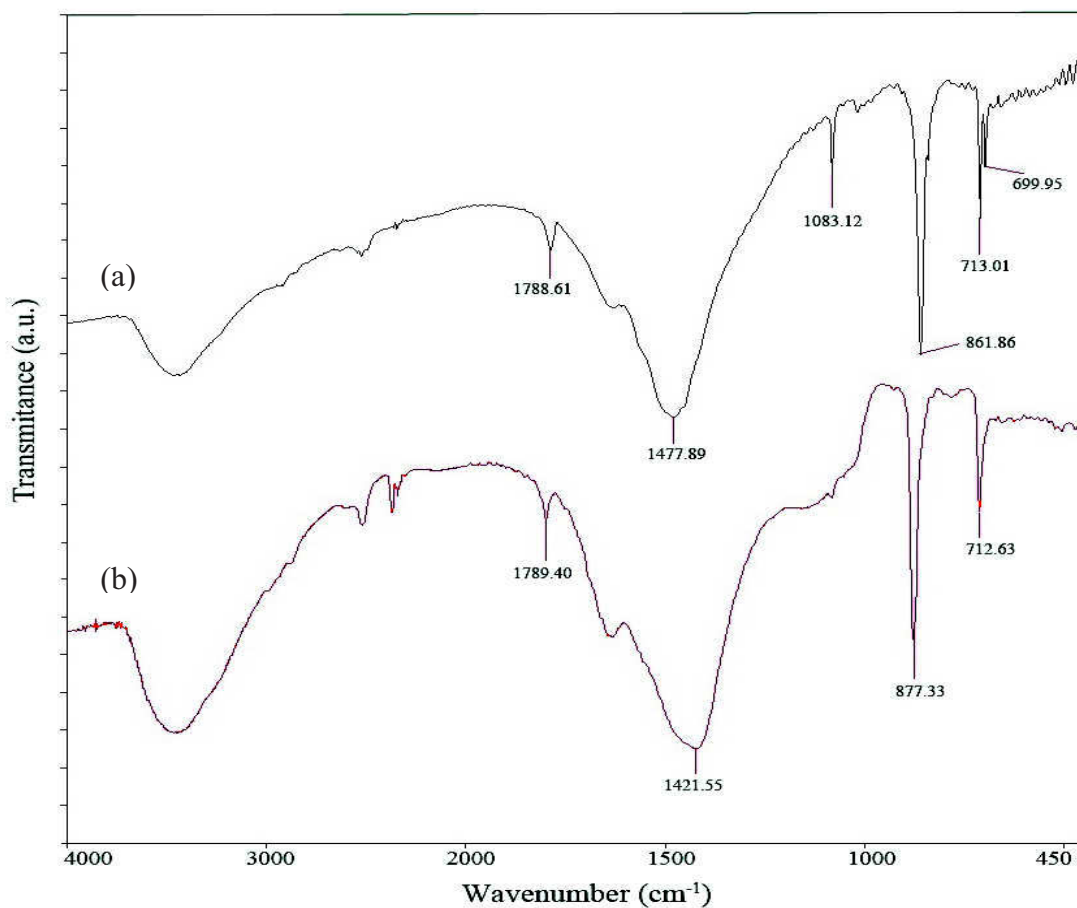
Figure 4.3 FT-IR spectra of (a) golden apple snail shell particles and
(b) oyster shell particles.

4.1.5 Thermogravimetric Analyzer, TGA

The thermogravimetric analysis curves of golden apple snail shells and oyster shells particles are shown in Figure 4.4. The degradation of golden apple snail and oyster shells occurred in two step. In the first step, the organic material and other oxide compound were decomposed at $300^{o}C$, respectively, and reduced the weight of approximately 2%. In step second step, the decrease start at $550^{o}C$ and ended at $850^{o}C$

with a weight loss of 55%. This decrease is ascribed to the burning of $CaCO_3$ to produce calcium oxide (CaO) and carbon dioxide (CO_2) about 42% by weight of the sample. Golden apple snail shell particles were composed of $CaCO_3$ 98.1135% and organic parts 1.8865% while oyster shell particles were composed of $CaCO_3$ 97.9502% and organic parts 2.0498%. The observed chemical composition of golden apple snail shells and oyster shells was entirely composed of $CaCO_3$ about 98%, which is in agreement with the XRF data [24].
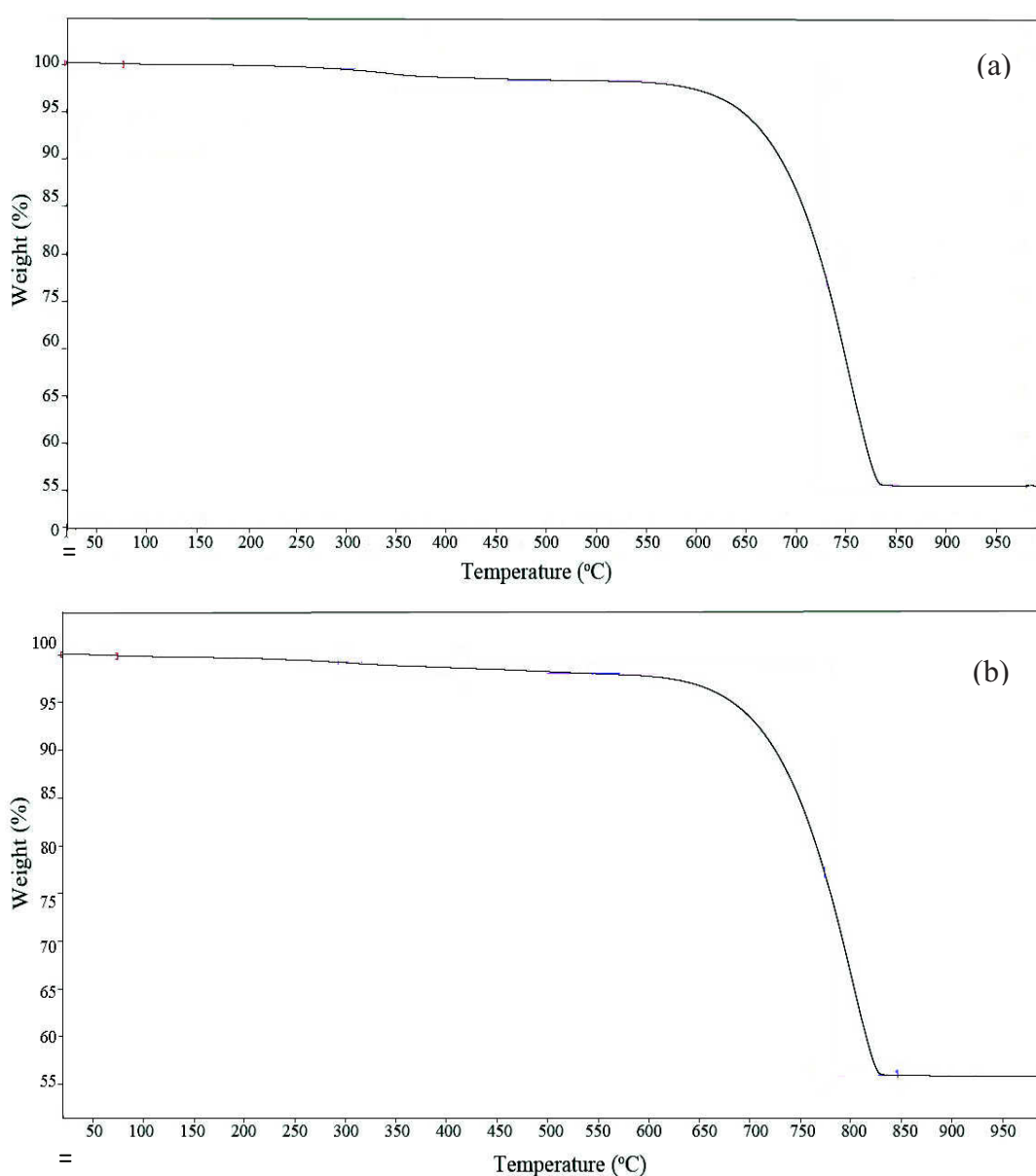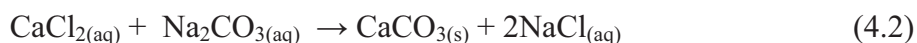

Figure 4.4 TGA thermogram of (a) golden apple snail shell particles and (b) oyster shell particles.

4.2 Mechanism for Nano-CaCO$_3$ Generation

Various techniques to synthesize CaCO$_3$ are emulsion membranes, lime soda process and solvay process. In this work, the solvay process is investigated because this technique is relatively simple. Precipitated CaCO$_3$ and a by-product are soluble salts, which can be easily eliminated and particle sizes of CaCO$_3$ are fairly uniform and can be varied from about 0.03-0.05 μm.

In solvay process, CaCO$_3$ from golden apple snail shells or oyster shells reacted with strong acid to produce calcium chloride (CaCl$_2$), carbon dioxide (CO$_2$) and water as seen in eq. 4.1. The slurry solution was filtered by filter paper No. 1 in order to remove the impurity and large particles of remained shells. CaCl$_2$ solution, the part of filter out, was then reacted with sodium carbonate (Na$_2$CO$_3$) to from CaCO$_3$ and sodium chloride (NaCl) as seen in eq. 4.2. Finally, precipitated CaCO$_3$ was washed to remove soluble salts [25].

$$CaCO_{3(s)} + 2HCl_{(aq)} \rightarrow CaCl_{2(aq)} + CO_{2(g)} + H_2O_{(l)} \qquad (4.1)$$

$$CaCl_{2(aq)} + Na_2CO_{3(aq)} \rightarrow CaCO_{3(s)} + 2NaCl_{(aq)} \qquad (4.2)$$

CaCl$_2$ and NaCl from solvay process were also indentified by XRD as shown in Figure 4.5(a) and (b). The precipitate CaCO$_3$ from golden apple snail shells and oyster shells after finishing solvay process were also indentified by XRD as shown in Figure 4.6(a) and (b). The precipitate CaCO$_3$ from golden apple snail shells after finishing solvay process was in vaterite form, while that of the precipitate CaCO$_3$ from oyster shells was a calcite form. The crystalline morphologies of golden apple snail shells and oyster shells after finishing solvay process were observed by a SEM and the results are shown in Figure 4.7(a) and (b). In Figure 4.7(a) the precipitate CaCO$_3$ from of golden apple snail shells after finishing solvay process was vaterite in the dipyramidal shape, while that of the precipitate CaCO$_3$ from oyster shells was calcite in cubic shape.
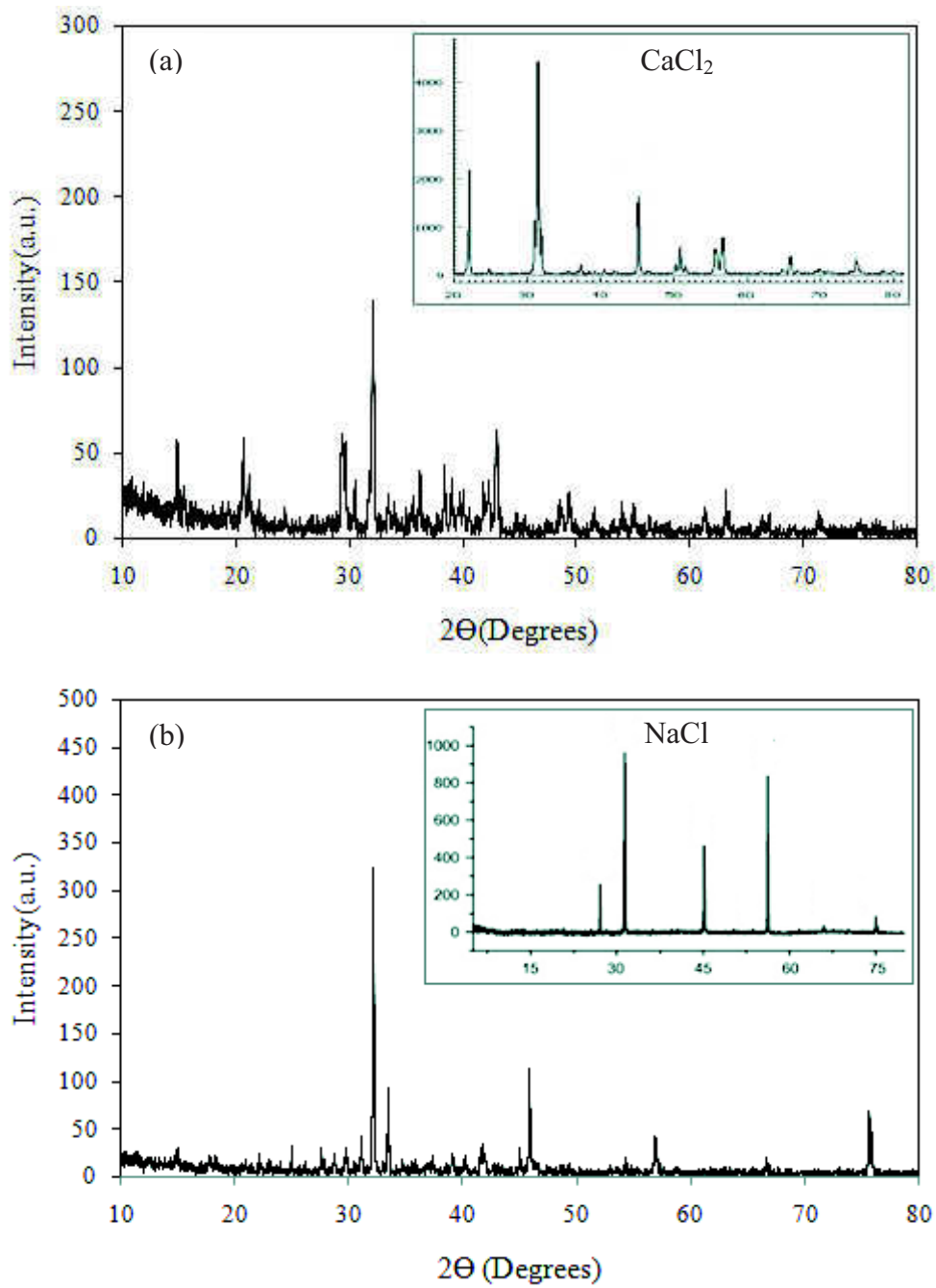
Figure 4.5 XRD patterns of (a) CaCl$_2$ and (b) NaCl from solvay process.
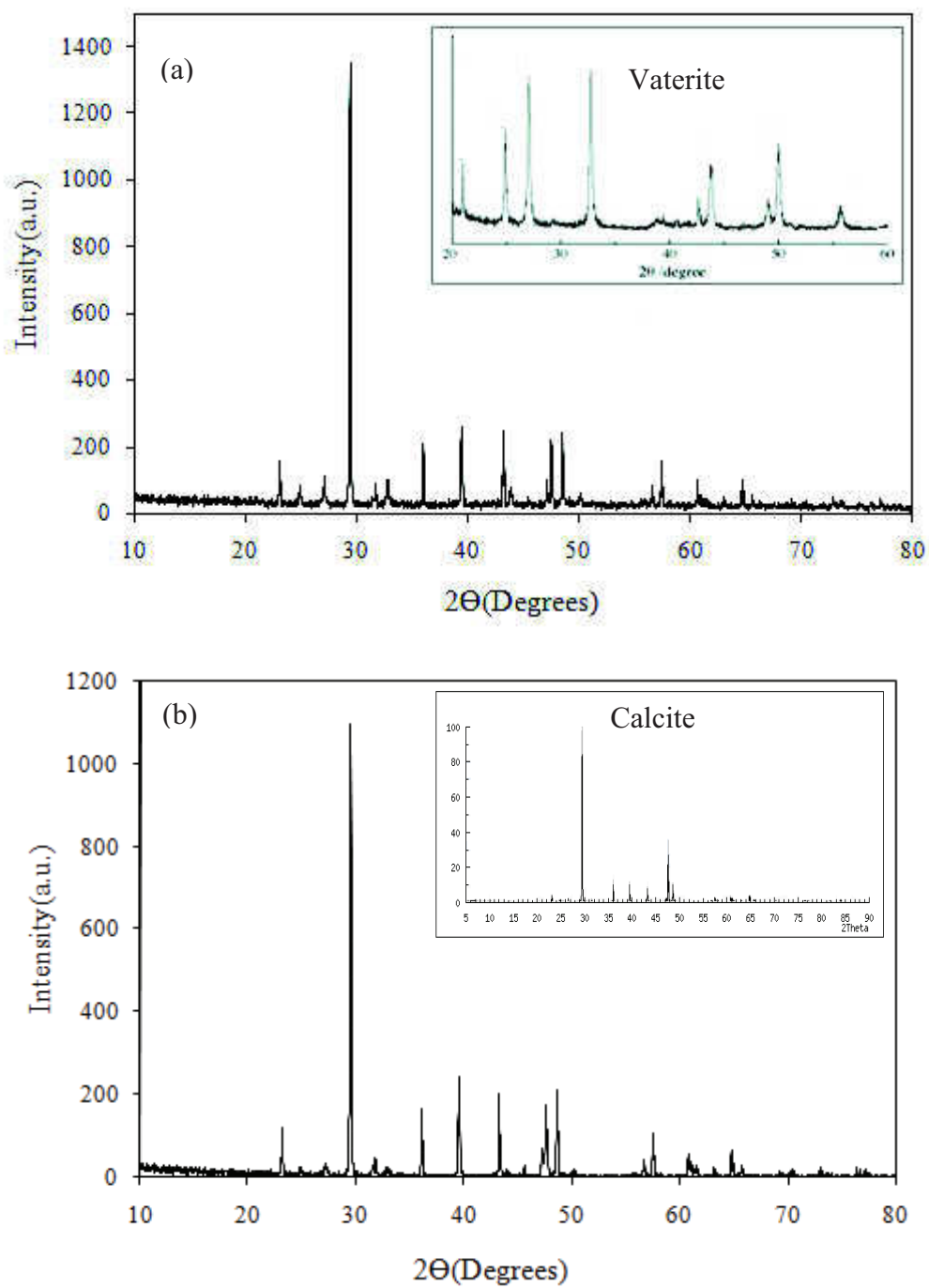
Figure 4.6 XRD patterns of the precipitate $CaCO_3$ (a) golden apple snail shells
(b) oyster shells after finishing solvay process.
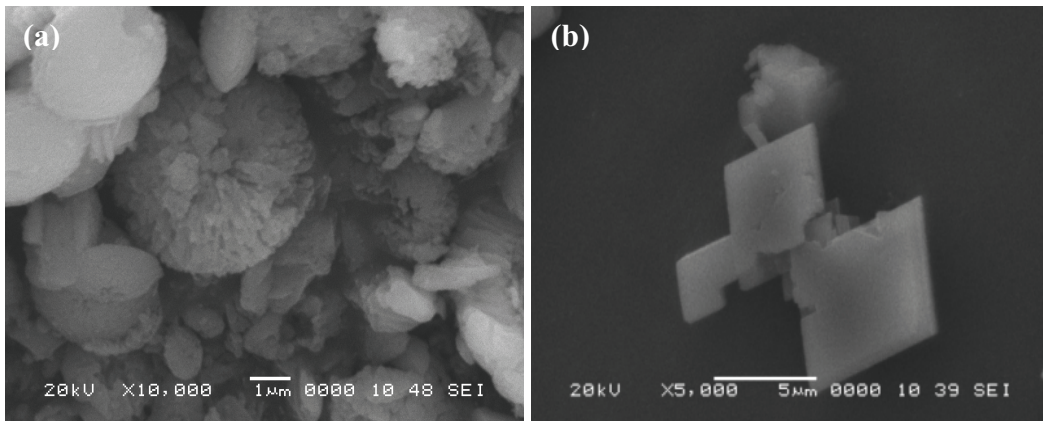
Figure 4.7 SEM images of the precipitate $CaCO_3$ (a) golden apple snail shells
(b) oyster shells after finishing solvay process.

The precipitated $CaCO_3$ by displacement reaction of $CaCl_2$ in Na_2CO_3 solution
was put in a teflon-lined stainless steel autoclave. The hydrothermal processing inside
the autoclave where high temperature-high pressure aqueous solution or vapor was
used as a transfer medium of heat, pressure and solvent which dissolves. These action
can also be use in processing of inorganic materials: preparation, formation,
alteration, sintering, etching. Particularly, the hydrothermal processing is suitable for
the preparation of powder; from nano-particles to single crystals.

4.3 Effect of Hydrothermal Reaction Temperature

4.3.1 X-Ray Diffraction, XRD

Figure 4.8 shows the XRD patterns of golden apple snail shells before hydrothermal process (a) and after hydrothermal processes at (b) 90°C, (c) 100°C, (d) 110°C, (e) 120°C and (f) 130°C for 20 h using Na_2CO_3 2 M. Before the hydrothermal process, $CaCO_3$ obtained from golden apple snail shells was in aragonite form. After the hydrothermal process (from 90°C to 130°C), the XRD patterns of $CaCO_3$ from golden apple snail shells showed the phase transition from aragonite to calcite forms. Usually, $CaCO_3$ in aragonite form is less common and less stable than calcite form.

Figure 4.9 shows the XRD patterns of oyster shells before hydrothermal process (a) and after hydrothermal processes at (b) 90°C, (c) 100°C, (d) 110°C, (e) 120°C and (f) 130°C for 20 h using Na_2CO_3 2 M. Before the hydrothermal process $CaCO_3$ obtained from oyster shells was in calcite form. After the hydrothermal process, the XRD patterns of $CaCO_3$ from oyster shells was in calcite form without any change of crystal structure. This is due to calcite form with trigonal symmetry is the most thermodynamically stable [26]. When the temperature of hydrothermal process increased. The peaks at 23.1° were rather sharp, which indicated that the calcite had relatively high crystallinity [27].

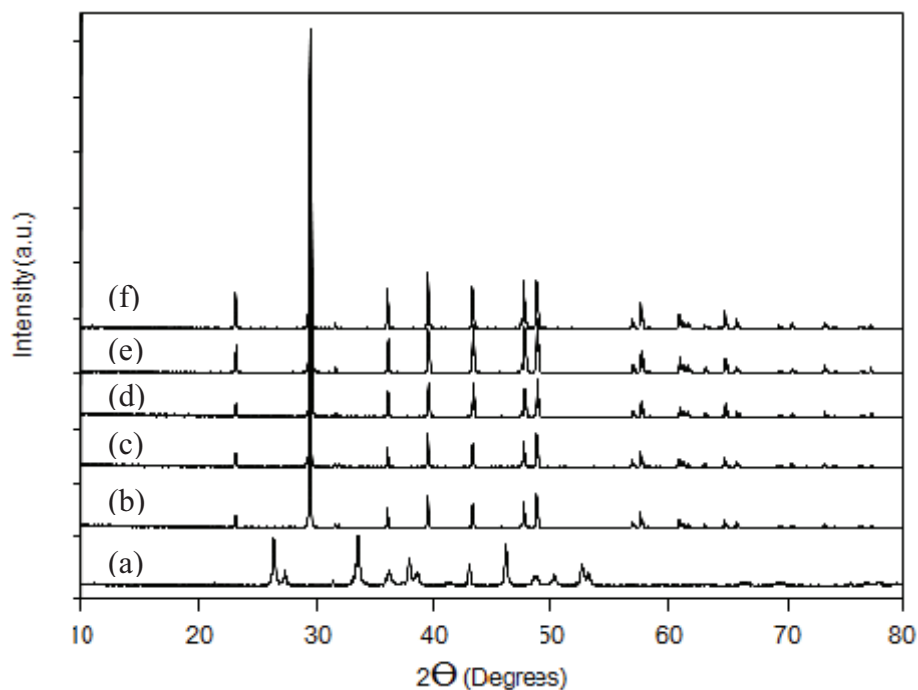Figure 4.8 XRD patterns of golden apple snail shells before hydrothermal
process (a) and after hydrothermal processes at (b) 90°C,
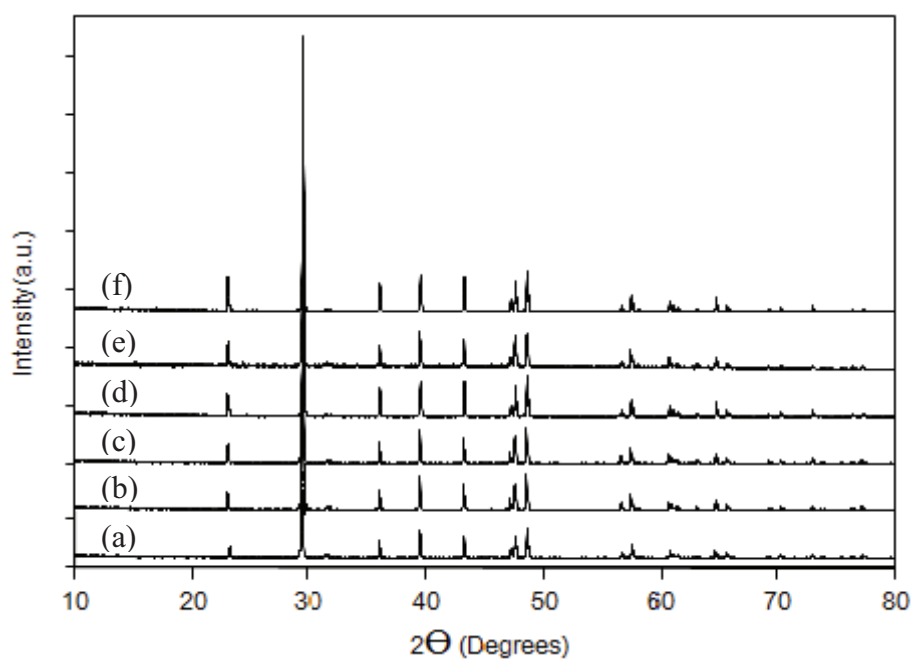(c) 100°C, (d) 110°C, (e) 120°C and (f) 130°C for 20 h.

Figure 4.9 XRD patterns of oyster shells before hydrothermal process (a)
and after hydrothermal processes at (b) 90°C, (c) 100°C, (d) 110°C,
(e) 120°C and (f) 130°C for 20 h.

4.3.2 Scanning Electron Microscopy, SEM

The morphologise of golden apple snail shells and oyster shells after hydrothermal processes at different temperatures were observed by a SEM as seen in Figure 4.10. The results are shown scalenohedral calcite as dominant morphology. The golden apple snail shells particles after hydrothermal process at 90 and 100°C for 20 h using Na_2CO_3 2 M was in calcite form with the particles size of 0.50-4.03 μm and 0.61-3.92 μm in width, while the increase of reaction temperature up to 130°C for 20 h, the particles size of $CaCO_3$ became larger about 3.90-7.50 μm in width.

The oyster shells particles after hydrothermal process at 90 and 100°C for 20 h using Na_2CO_3 2 M was in calcite form with particles size of 0.50-3.93 μm and 0.41-2.51 μm in width, while the increase of reaction temperature up to 130°C for 20 h, the particles size of $CaCO_3$ became larger about 0.70-2.01 μm in width. Under the condition of hydrothermal process at 90°C, particle sizes of $CaCO_3$ from golden apple snail shells or oyster shells were similar to those at 100°C. Unfortunately, at 90°C, the recrystallization of $CaCO_3$ was not completed. When the temperature increased up to 130°C, the recrystallization of $CaCO_3$ was completed, resulting in the larger particle size of $CaCO_3$. It is because at high temperature $CaCO_3$ particles trended to be aggregated and agglomerates together due to the loss of moisture or solvent [28].
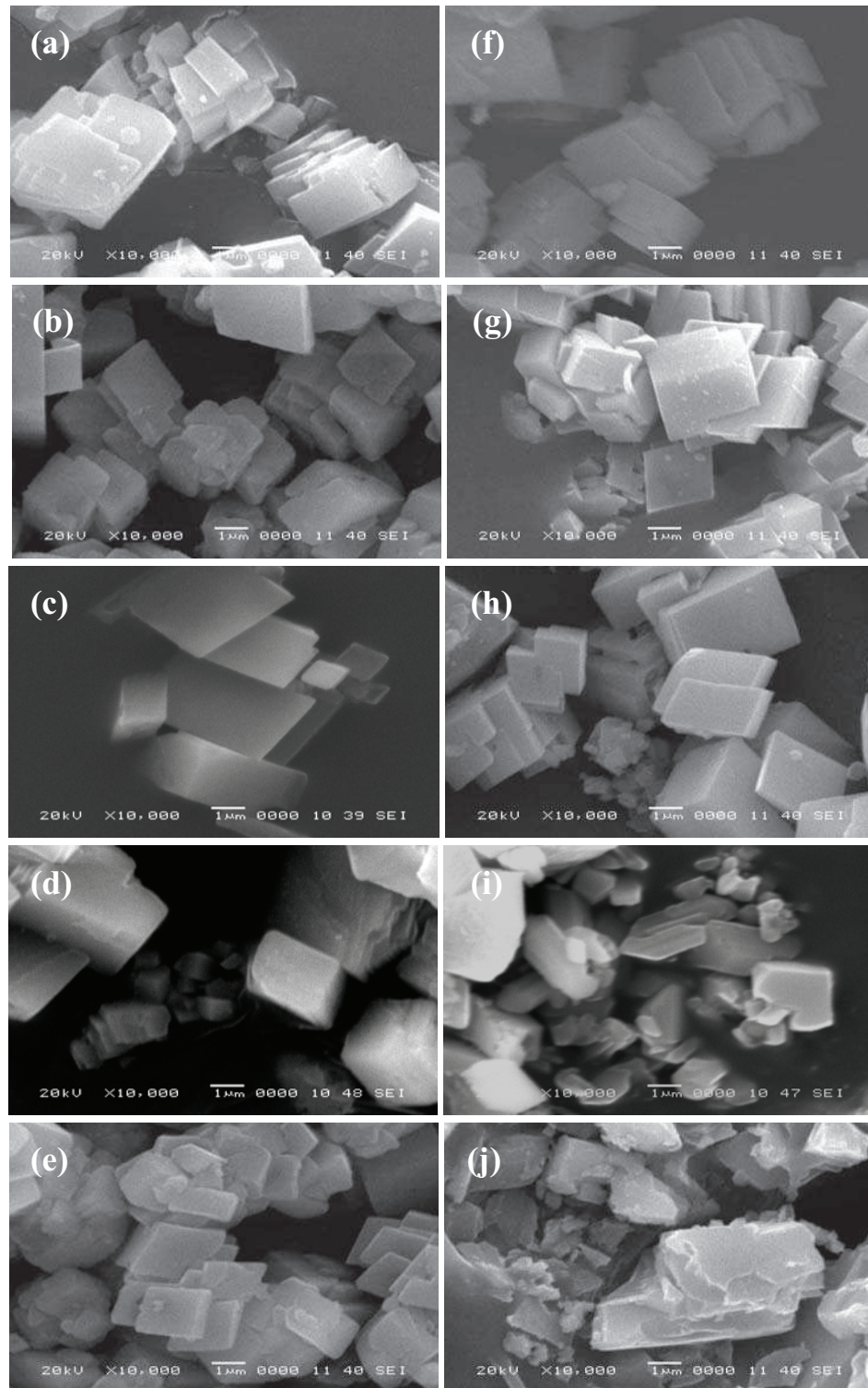
Figure 4.10 SEM images of golden apple snail shells after hydrothermal

process for 20 h at (a) 90°C, (b) 100°C, (c) 110°C, (d) 120°C,

(e) 130°C and oyster shells after hydrothermal process for 20 h at

(f) 90°C, (g) 100°C, (h) 110°C, (i) 120°C, (j) 130°C, respectively.

4.4 Effect of Concentration of Na$_2$CO$_3$

4.4.1 Scanning Electron Microscopy, SEM

Figure 4.11 shows the morphologise of golden apple snail shells after hydrothermal processes at 100°C for 20 h using Na$_2$CO$_3$ 1 M and 3 M. The CaCO$_3$ particle sizes of golden apple snail shells after hydrothermal process at 100°C for 20 h using Na$_2$CO$_3$ 1M were about 0.49-3.81 μm in width. When the concentration of Na$_2$CO$_3$ increased up to 3 M, the particle size of CaCO$_3$ was about 0.41-2.51 μm in width. As seen in Figure 4.11 (a) and (b). The CaCO$_3$ particle sizes of oyster shells after hydrothermal process at 100°C for 20 h using Na$_2$CO$_3$ 1 M were about 0.68-2.24 μm in width. When the concentration of Na$_2$CO$_3$ increased up to 3 M, the particle size of CaCO$_3$ was about 0.29-1.95 μm in width. Accordingly, particle size were independent of Na$_2$CO$_3$ concentration. The particle size of CaCO$_3$ did not increase with increasing concentration of Na$_2$CO$_3$. Additionlly, the increase of Na$_2$CO$_3$ concentration caused the increase of CaCO$_3$ yield [28]. The result of % yield of CaCO$_3$ from golden apple snail shells and oyster shells after hydrothermal process at various concentration of Na$_2$CO$_3$ was shown in Table 4.2.

Table 4.2 The result of % yield of CaCO$_3$ from golden apple snail shells and oyster
shells after hydrothermal process.

Sample		Hydrothermal condition			A-HT weight	% Yield
Type	Weight	Conc. Na$_2$CO$_3$ (M)	Temp (^{o}C)	Time (h)		
GB	100.1469	1	100	20	72.1370	72.0312
GB	100.7289	2	100	20	86.4718	85.8460
GB	100.6801	3	100	20	90.0641	89.4557
OB	100.1872	1	100	20	73.6652	73.5275
OB	100.0419	2	100	20	85.512	84.4766
OB	100.5183	3	100	20	89.1096	88.6501

GB, golden apple snail shell particles.
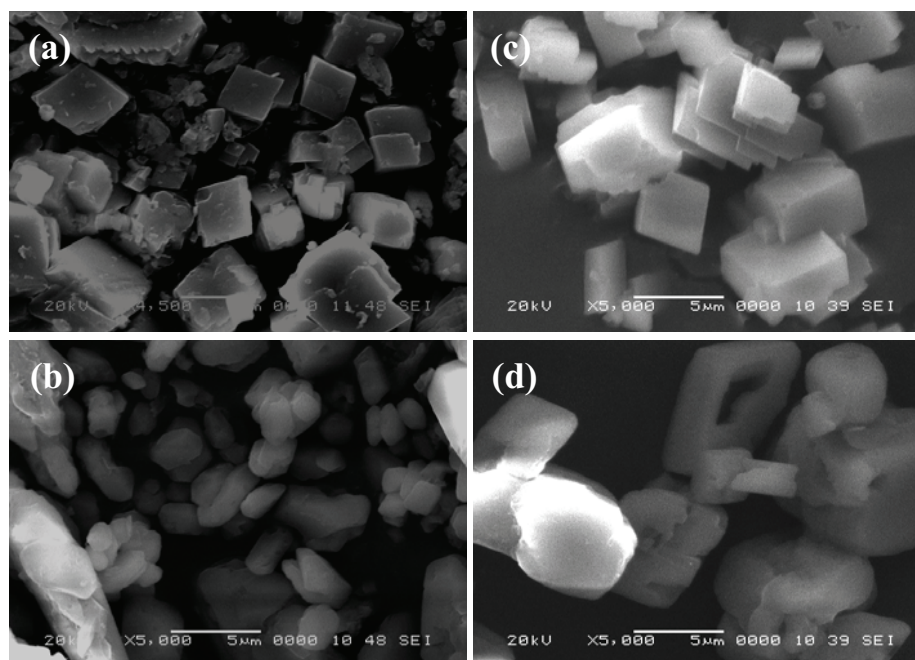OB, oyster shell particles.
A-HT, after hydrothermall process.

Figure 4.11 SEM images of (a) golden apple snail shells after hydrothermal
process at 100^oC for 20 h, Na_2CO_3 1 M, (b) Na_2CO_3 3 M and of
(c) oyster shells after hydrothermal process at 100^oC for 20 h,
Na_2CO_3 1 M (d) Na_2CO_3 3 M, respectively.

4.5   Effect of Hydrothermal Reaction Time

4.5.1   X-Ray Diffraction, XRD

Figure 4.12 shows the XRD patterns of golden apple snail shells after
solvay process and after hydrothermal processes at 100^oC for various time. As
discussion in section e.q. 4.2, the precipitate $CaCO_3$ after finishing solvay process was
in vaterite. As it is less stable than either calcite and can be synthesized from a
chemical reaction. Vaterite and aragonite were not identified during the hydrothermal
process, when increaseing hydrothermal temperature reaction at 100^oC for at various
time $CaCO_3$ were recrystallized from vaterite to calcite. This is due to vaterite or
aragonite is less common and less stable than calcite, while the $CaCO_3$ calcite form
with trigonal symmetry is the most thermodynamically stable form of pure $CaCO_3$ at
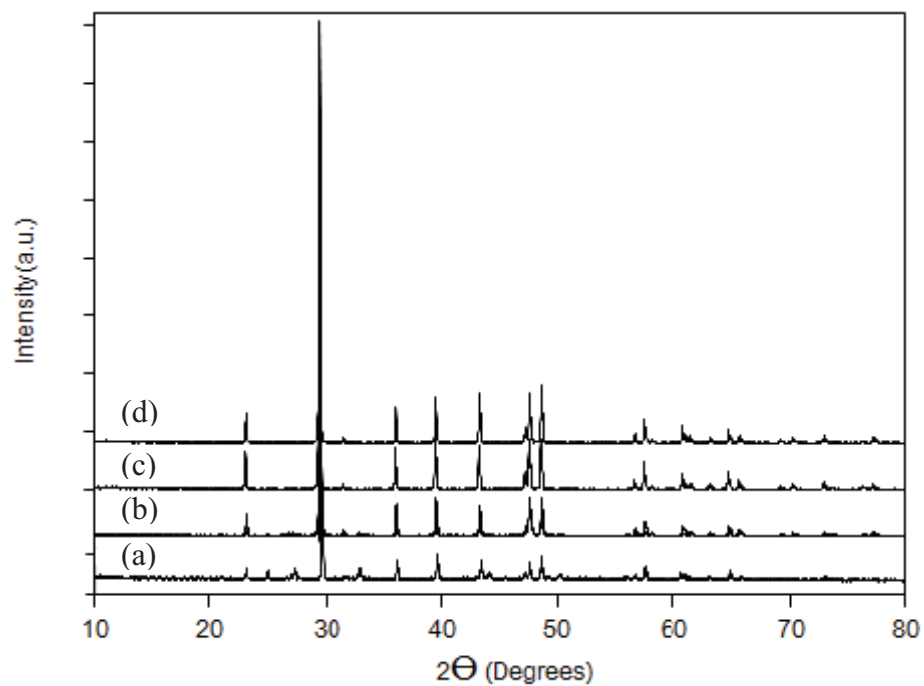room temperature under atmospheric pressure [28-29].

Figure 4.12 XRD patterns of golden apple snail after solvay process (a)
and after hydrothermal processes at 100°C for (b) 1 h, (c) 10 h,
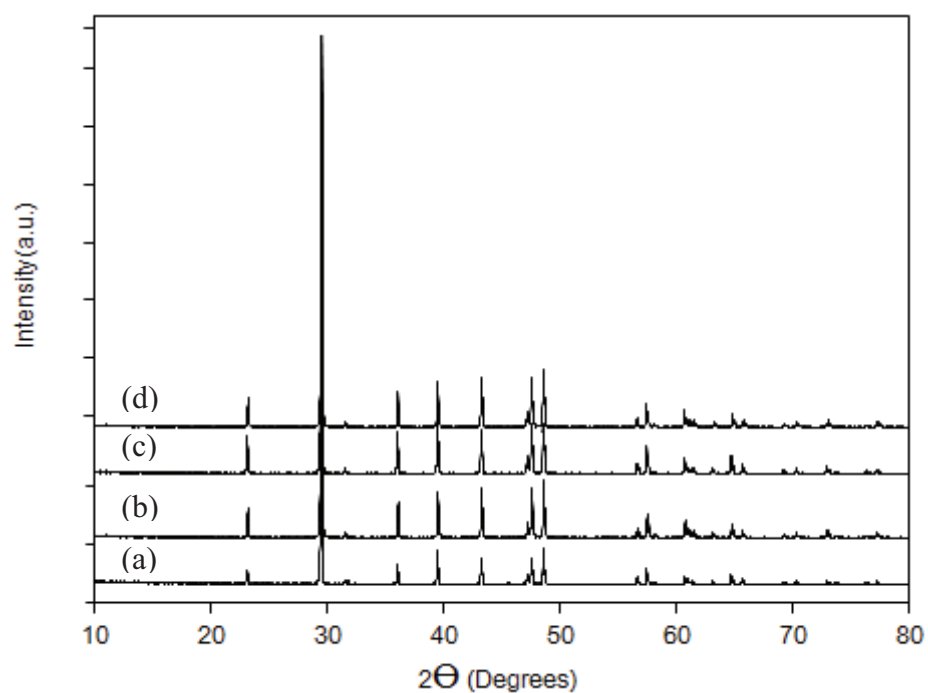(d) 20 h.

Figure 4.13 XRD patterns of oyster shell after solvay process (a) and after
hydrothermal processes at 100°C for (b) 1 h, (c) 10 h, (d) 20 h.

Figure 4.13 shows the XRD patterns of oyster shells after solvay process and after hydrothermal processes at 100°C for various time. The crystalline phase of $CaCO_3$ after the successive chemical reaction was in calcite form and the $CaCO_3$ was in calcite form without any change of crystal structure after hydrothermal process at 100°C for different reaction time.

4.5.2   Transmission Electron Microscopy, TEM

Figure 4.14 shows TEM images of $CaCO_3$ particles obtained from golden apple snail after hydrothermal process at 100°C for 1 h. The particles size was in the range of 30-850 nm in width. When the reaction time increased up to 10 h, the particles size of $CaCO_3$ became larger about 500-4030 nm in width. The $CaCO_3$ particles obtained from oyster shells after hydrothermal process at 100°C for 1 h were about 74-246 nm in width. When the reaction time increase up to 10 h, the particles size of $CaCO_3$ became larger about 290-1150 nm in width. The increase of reaction time in the reactor leaded not only to an aggregation of $CaCO_3$ particles but also $CaCO_3$ particles trended to be migration among CaCO3 crystallines [28-29]. The result of particles size of $CaCO_3$ from golden apple snail shells and oyster shells after hydrothermal process at various conditions was shown in Table 4.3.
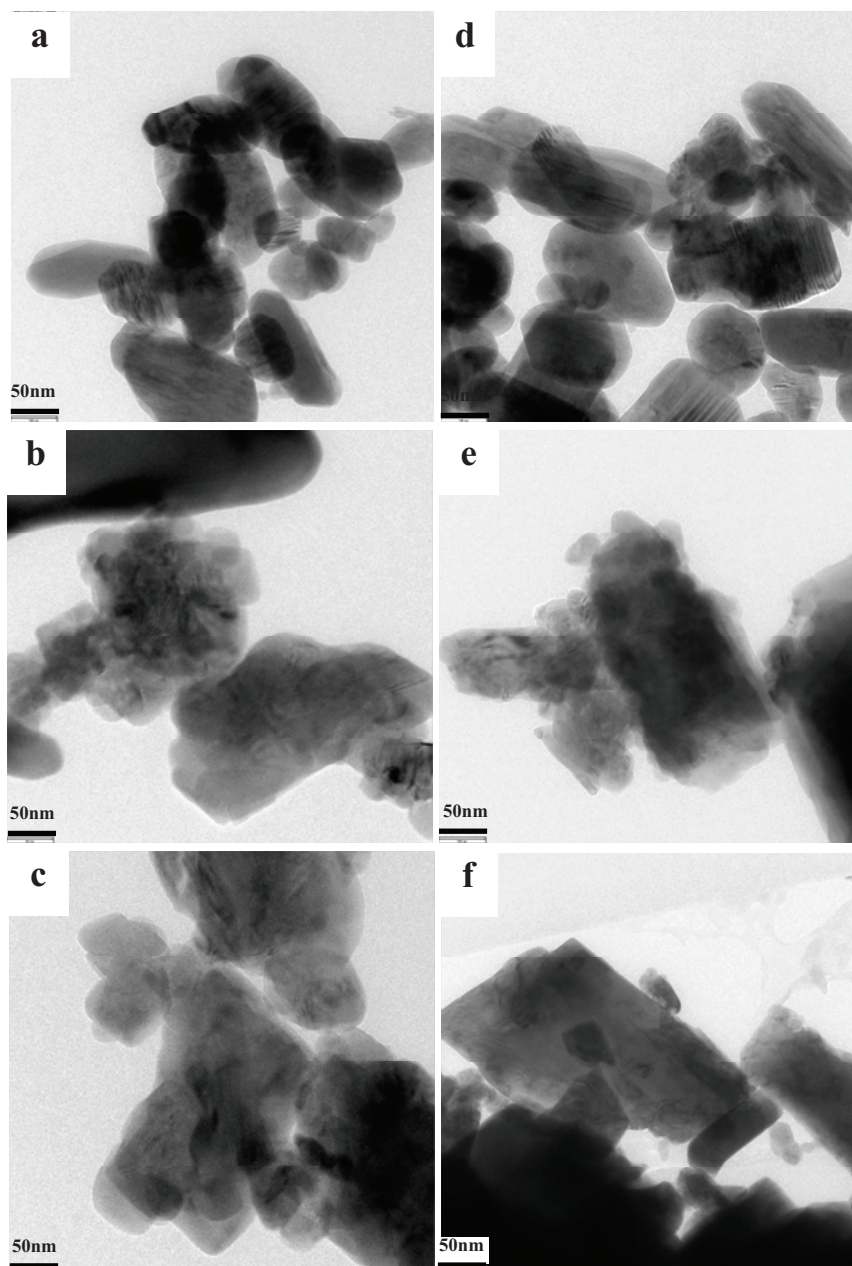
Figure 4.14 TEM images of golden apple snail after hydrothermal process at
100°C for (a) 1 h, (b) 10 h and (c) 20 h and oyster shell after
hydrothermal process at 100°C for (a) 1 h, (b) 10 h and (c) 20 h,
respectively.

Table 4.3 The result of particles size of $CaCO_3$ from golden apple snail shells and oyster shells after hydrothermal process.

Sample	Reaction temperature (^{o}C)	Conc. Na_2CO_3 (M)	Reaction time (h)	XRD crystal structure[a]	Particle size[b] (nm)
GB	-	-	-	Aragonite	650-7,870
GS	-	-	-	Vaterite	340-3660
GA	90	2	20	Calcite	500-4,030
GA	100	1	20	Calcite	490-3,810
GA	100	2	1	Calcite	30-850
GA	100	2	10	Calcite	500-4,030
GA	100	2	20	Calcite	610-3,920
GA	100	3	20	Calcite	680-2,240
GA	110	2	20	Calcite	1,190-4,070
GA	120	2	20	Calcite	2,023-5,440
GA	130	2	20	Calcite	3,900-7,500
OB	-	-	-	Calcite	970-7,650
OS	-	-	-	Calcite	410-2290
OA	90	2	20	Calcite	500-3,930
OA	100	1	20	Calcite	680-2,240
OA	100	2	1	Calcite	74-246
OA	100	2	10	Calcite	290-1,150
OA	100	2	20	Calcite	410-2,510
OA	100	3	20	Calcite	290-1,950
OA	110	2	20	Calcite	490-2,500
OA	120	2	20	Calcite	650-1,400
OA	130	2	20	Calcite	700-2,010

[a]X-ray diffiration (XRD).
[b]Scanning electron microscope (SEM).
GB, golden apple snail shell particles.
GS, golden apple snail shells after solvay process.
GA, golden apple snail shells after hydrothermal process.
OB, Oyster shell particles.
OS, Oyster shells after solvay process.
OA, Oyster shells after hydrothermal process.

4.5.3 X-Ray Fluorescence, XRF

Table 4.4 shows the chemical composition of golden apple snail and oyster shells under the optimum condition hydrothermal process at 100^oC for 1 h using Na_2CO_3 2 M. Golden apple snail shell particles after hydrothermal process at 100^oC for 1 h was entirely composed of $CaCO_3$ about 99% and other oxide compounds about 1%, while that of oyster shell particles were entirely composed of $CaCO_3$ about 98% and other oxide compounds about 2%, respectively. The chemical composition of $CaCO_3$ from golden apple snail shells under the optimum condition hydrothermal process at 100^oC for 1 h was similar to those of golden apple snail particles. The $CaCO_3$ from oyster shells under the optimum condition of hydrothermal process at 100^oC for 1 h was purified more than oyster shells particles.

Table 4.4 Chemical composition of golden apple snail shells and oyster shells before and after hydrothermal process at 100^oC for 1 h, Na_2CO_3 2 M by XRF.

Sample	Chemical composition (%)										
	$CaCO_3$	Na_2O	Al_2O_3	SiO_2	P_2O_5	SO_3	Cl	K_2O	MaO_2	Fe_2O_3	SrO
G-BHP[1]	99.302	0.307	0.033	0.126	0.021	0.044	0.015	0.022	0.069	0.050	0.011
G-AHP[2]	99.026	0.676	-	0.017	-	0.011	0.108	-	0.054	0.023	-
O-BHP[3]	96.715	0.829	0.313	0.964	0.143	0.460	0.376	0.052	-	0.122	0.027
O-AHP[4]	98.077	0.926	-	0.018	0.014	0.161	0.299	-	0.054	0.023	-

[1]Golden apple snail shell particles before hydrothermal process.

[2]Golden apple snail shell particles after hydrothermal process at 100^oC for 1 h.

[3]Oyster shell particles before hydrothermal process.

[4]Oyster shell particles after hydrothermal process at 100^oC for 1 h.

4.5.4   Fourier Transform Infrared Spectroscopy, FT-IR

The results were further demonstrated by FT-IR of $CaCO_3$ from golden apple snail shells under the optimum condition of hydrothermal process at 100^oC for 1 h using concentration of Na_2CO_3 2 M as shown in Figure 4.15. FT-IR is very useful tool for the identification of $CaCO_3$ polymorphs. Under the optimum of condition hydrothermal process at 100^oC for 1 h, Na_2CO_3 2 M, $CaCO_3$ from golden apple snail was recrystallized from aragonite to calcite. It can be seen that golden apple snail before hydrothermal process shown in Spectrum (a), the vibrational bands at about 1083.43 and 861.97 cm^{-1} could be assigned to the characteristic symmetric carbonate stretching (v_1 mode) and carbonate out-off-plane bending (v_2 mode) vibration of aragonite. Additionally, the spectrum of $CaCO_3$ obtained from golden apple snail under the optimum hydrothermal process (100^oC, 1 h, Na_2CO_3 2 M) is shown in Figure 4.15 (b). The bands at 875.85 and 712.17 cm^{-1} could be attributed to the out-off-plane bending (v_2 mode) and carbonate in-plane-bending (v_4 mode) of calcite [29].
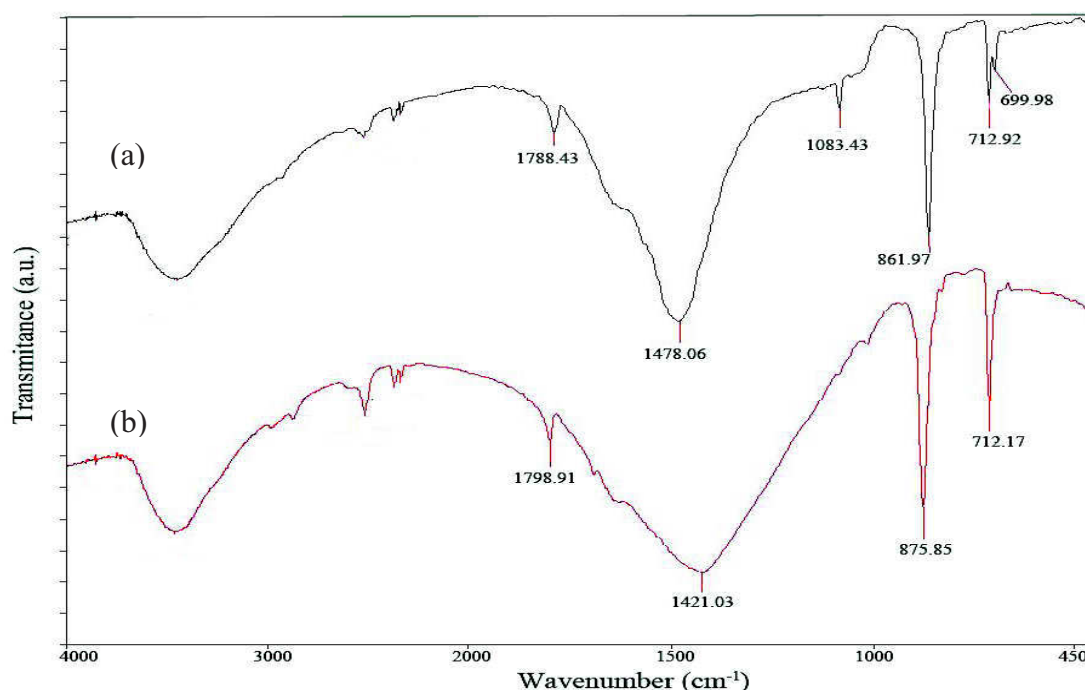

Figure 4.15 FT-IR spectra of golden apple snail shells (a) and (b) golden apple snail shells under the optimum condition of hydrothermal process at 100^oC for 1 h, Na_2CO_3 2 M.

Additionally, the results were further demonstrated by FT-IR of $CaCO_3$ from oyster shells under the optimum condition of hydrothermal process at 100^oC for 1 h, Na_2CO_3 2 M, as given in Figure 4.16. $CaCO_3$ from oyster shells before and after hydrothermal process was in calcite form without any change of crystal structure after hydrothermal process, showed in Figure 4.16 (a) and (b), the bands at 877.33 and 875.13 cm^{-1} can be attributed to the out-off-plane bending and the bands at 712.63 and 718.64 cm^{-1} can be attributed to the carbonate in-plane-bending modes of calcite. In addition, a weak peak about 1421.25 and 1420.86 cm^{-1} could be assigned to the stretching vibration of C=O band in carboxylate of $CaCO_3$ [29].
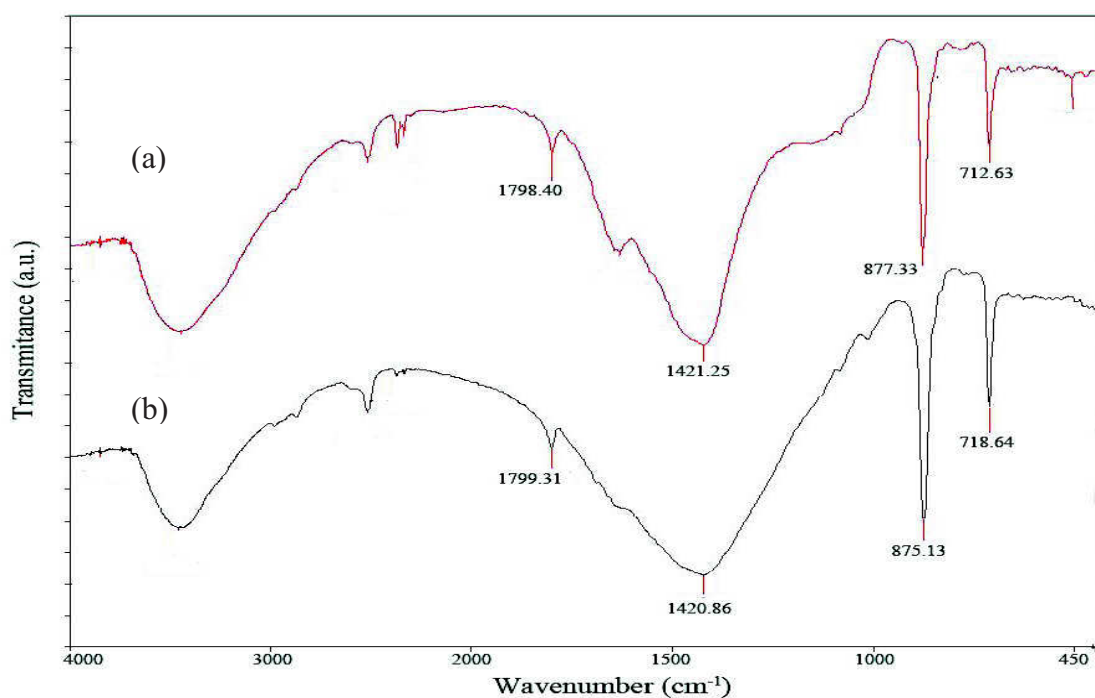

Figure 4.16 FT-IR spectra of oyster shells (a) and (b) oyster shells under the optimum condition of hydrothermal process at 100^oC for 1 h, Na_2CO_3 2 M.

4.5.5 Thermogravimetric Analyzer, TGA

The thermogravimetric analysis curves of golden apple snail shell and oyster shell particles under the optimum condition of hydrothermal process at 100°C for 1 h are shown in Figure 4.17. Figure 4.17(a) showed the degradation occurred in two steps. In the first step, the decomposition of organic material and other oxide took place at 300°C and reduced the weight of approximately 0.5%. In step second step, the decrease start at 530°C and ended at 850°C with a weight loss of 56%. This decrease was ascribed to the burning of $CaCO_3$ to produce calcium oxide (CaO) and carbon dioxide (CO_2) about 43% by weight of the sample. Golden apple snail shell particles under the optimum condition of hydrothermal process at 100°C for 1 h were composed of $CaCO_3$ 99.4651% and organic parts 0.5349%. Therefore, the degradation temperature in the first step of golden apple snail shell particles (350°C) was higher than that of golden apple snail shell particles under the optimum condition of hydrothermal process (300°C). It is because the golden apple snail shell particles under the optimum condition of hydrothermal process was composed of sodium chloride (about 0.783%) more than golden apple snail shell particles and its decomposed at around 300°C [30].

In contrast, in Figure 4.17(b), the degradation of oyster shell particles under the optimum condition of hydrothermal process at 100°C for 1 h occurred in two steps. In the first step, the organic material and other oxide compound were decomposed at 300°C, respectively, and reduced the weight of approximately 1%. In step second step, the decrease start at 550°C and ended at 850°C with a weight loss of 56%. This decrease was ascribed to the burning of $CaCO_3$ to produce CaO and CO_2 about 43% by weight of the sample. Oyster shell particles under the optimum condition of hydrothermal process at 100°C for 1 h were composed of $CaCO_3$ 98.9089% and organic parts 1.0991%. The degradation temperature of $CaCO_3$ from oyster shell particles under the optimum condition hydrothermal process at 100°C for 1 h was similar to those of oyster shells particles.

The observed chemical composition of golden apple snail shells and oyster shells was entirely composed of $CaCO_3$ about 99%, which is in agreement with the XRF data.
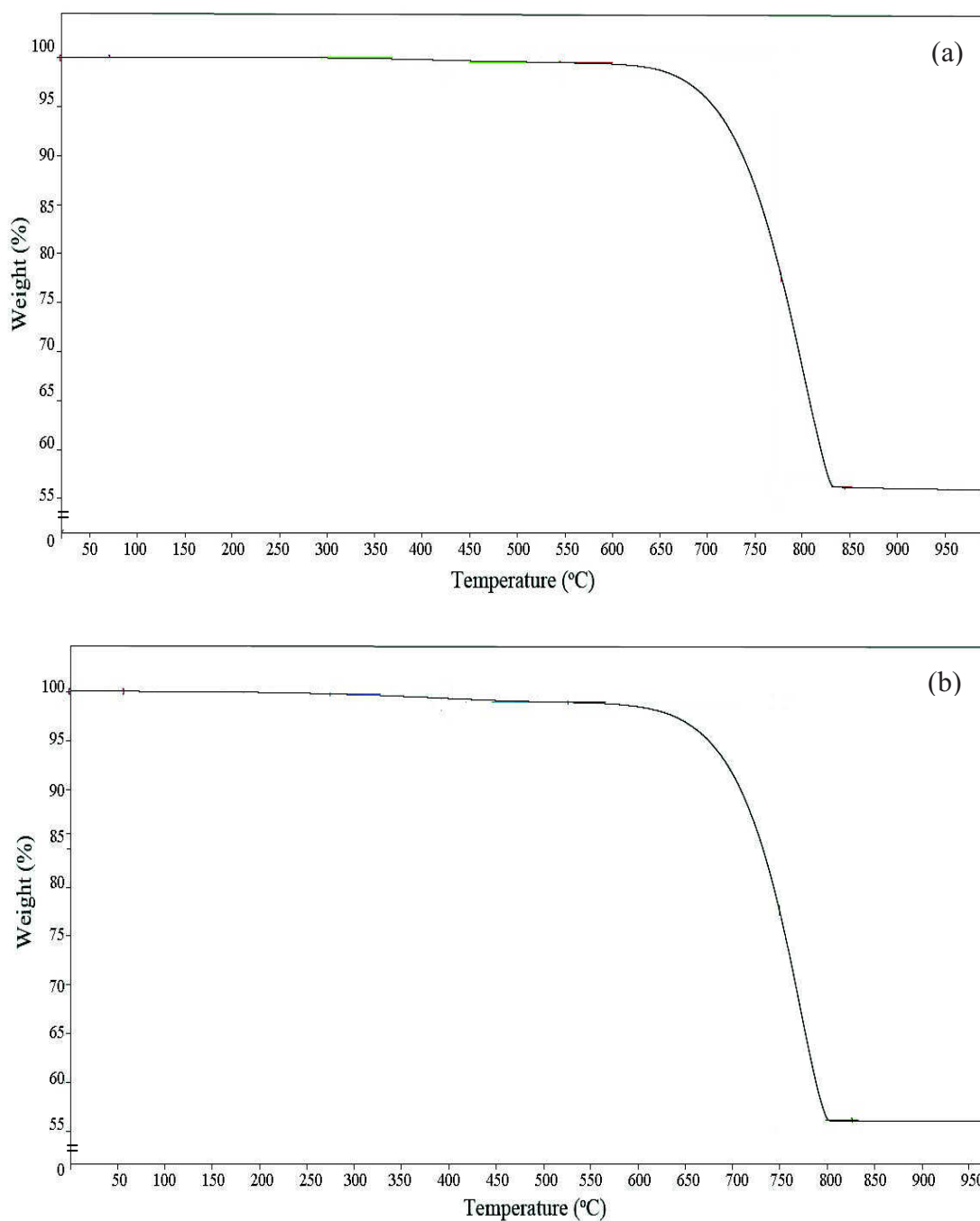
Figure 4.17 TGA thermogram of golden apple snail shell and oyster shell particles under the optimum condition of hydrothermal process at 100°C for 1 h, Na_2CO_3 2 M.

4.6   Morphological, Mechanical Properties and Thermal Properties of PVC Composite Materials

4.6.1   Mechanical Properties

The mechanical properties of PVC composites materials were shown in Figures 4.18-4.21. The tensile strength (T_B) of PVC composite materials slightly decreased with the increase of $CaCO_3$ contents as seen in Figure 18. By using 5 phr $CaCO_3$ from golden apple snail shells under the optimum condition of hydrothermal process at 100^oC for 1 h (GA), the maximun value of T_B was 36.3 MPa and by using 5 phr $CaCO_3$ from oyster shells under the optimum condition of hydrothermal process at 100^oC for 1 h (OA), the maximun value of T_B was 36.1 MPa. It is clearly seen that by adding GA and OA, T_B of PVC composite material were improved compared with not only neat PVC but also $CaCO_3$ from golden apple snail shells particles (GB) and $CaCO_3$ from oyster shells particles (OB) filled with PVC. It indicated that the $CaCO_3$ nanoparticle under the optimum condition of hydrothermal process at 100^oC for 1 h can improve the mechanical properties of PVC composite materials, especially the tensile strength. In Figure 4.18(b) shown T_B of PVC composite materials, when adding 5 phr $CaCO_3$ from nano-$CaCO_3$ commercial grade (B800) and micro-$CaCO_3$ commercial grade (OMYA-2) filled PVC showed maximun value at 36.8 MPa and 36.7 MPa. The T_B of PVC composite materials using 5 phr $CaCO_3$ from GA and OA were almost comparable with the commercial $CaCO_3$. The T_B of nano-$CaCO_3$ filled PVC is higher than that of micro-$CaCO_3$ filled PVC due to the nano-$CaCO_3$ filled PVC, with larger interfacial area, had higher ultimate tensile strength than micro-$CaCO_3$.

Figure 4.19(a) showed the elongation at break of PVC composites materials. the elongation at break (E_B) of PVC composite materials slightly decreased with the increase of $CaCO_3$ contents. By using 5 phr $CaCO_3$ from GA, the maximun value of E_B was 198.1% and by using 5 phr $CaCO_3$ from OA, the maximun value of E_B was 193.3%. Figure 4.19(b) shows E_B of PVC composite materials, when adding 5 phr $CaCO_3$ from B800 and OMYA-2 particles filled PVC showed maximum value at 202.2% and 202.0%. The E_B of PVC composite materials using 5 phr $CaCO_3$ from

GA and OA were lower than those of B800 and OMYA-2 particles. It is may be due to not only the different surface properties of $CaCO_3$ but also the particle size of $CaCO_3$.

Figure 4.20 (a) and (b) showed the hardness of PVC composite materials seemed to be increased with increasing filler loading and its value of composite material was higher than that of neat PVC when filler was added more than 10 phr.

Figure 4.21 shown the izod impact strength of PVC composites materials. The izod impact strength of PVC composite materials slightly decreased with the increased of $CaCO_3$ content. When adding 5 phr $CaCO_3$ from GA and OA, the izod impact strength reached 75.53 J/M^2 and 76.34 J/M^2. It is clearly seen that by adding GA and OA, the izod impact strength of PVC composite material were improved compared with not only neat PVC (69.02 J/M^2) and $CaCO_3$ from GB (71.99 J/M^2) and $CaCO_3$ from OB (71.71 J/M^2). Figure 4.19(b) shows izod impact strength of PVC composite materials, when adding 5 phr from B800 and OMYA-2 particles filled PVC showed maximum value at 74.67 J/M^2 and 75.72 J/M^2. Clearly nano-sized $CaCO_3$ had an effective toughening effect on the PVC composite. This results the great advantage of using nano-$CaCO_3$ as strengthening fillers in polymer processing. The first reason for higher tensile and impact strength of nano-$CaCO_3$ filled PVC composites is that nano-$CaCO_3$ had larger surface area and so larger interfacial area with the polymer matrix. As such, the overall bonding strength between the particle and matrix was higher. Thus, it is to be expected that the composites could stand higher loading under external forces. Secondly, it is well accepted that cavitation and cavitation-induced shear yielding is the dominant mechanism of the toughening of particulate filled polymers [31-32].

The result for the effect of $CaCO_3$ nanoparticles and microparticles on mechanical properties of PVC rigid profile application. The mechanical properties of PVC rigid profile produced in golden apple snail shell and oyster shell particles under the optimum condition of hydrothermal process at $100^{\circ}C$ for 1 h were significantly improved after addition of 5 phr of nano-$CaCO_3$. However, due to the presence of nano-$CaCO_3$, the profile could get good mechanical properties with a small quantity of $CaCO_3$.
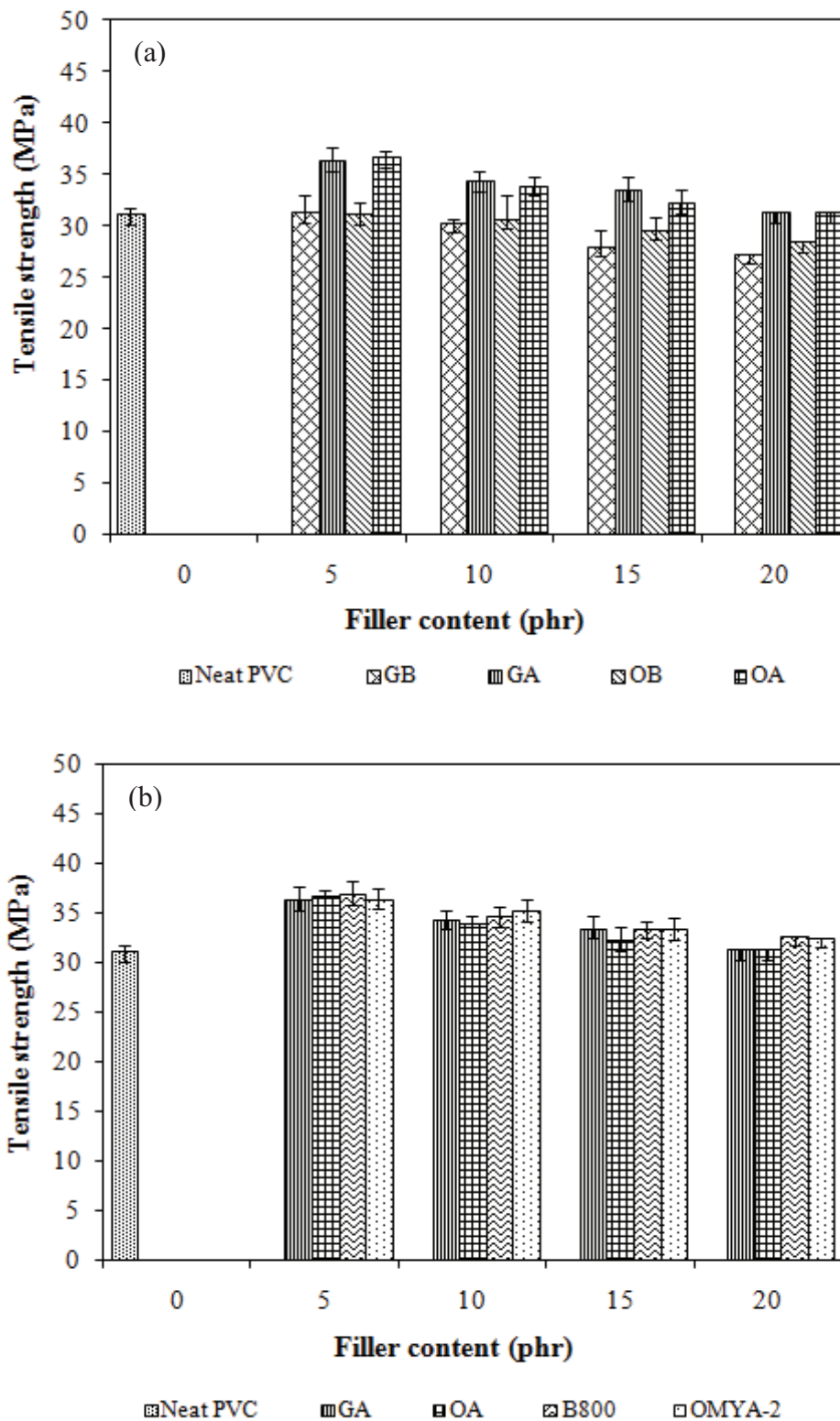
Figure 4.18 Tensile strength of PVC composites (a) neat PVC, GB, GA,
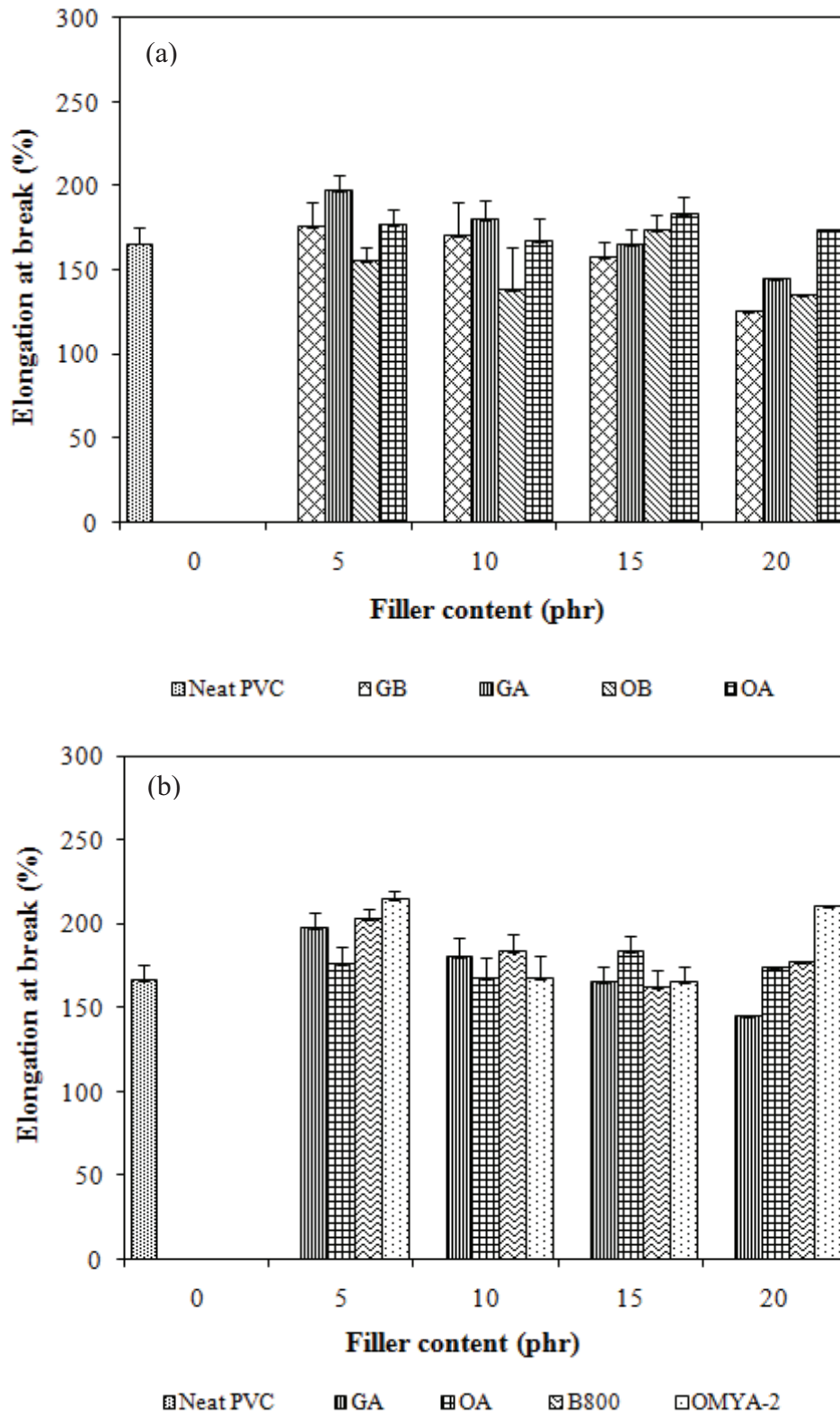OB and OA, (b) neat PVC, GA, GA, B800 and OMYA-2.

Figure 4.19 Elongation at break of PVC composites (a) neat PVC, GB, GA, OB and OA, (b) neat PVC, GA, OA, B800 and OMYA-2.
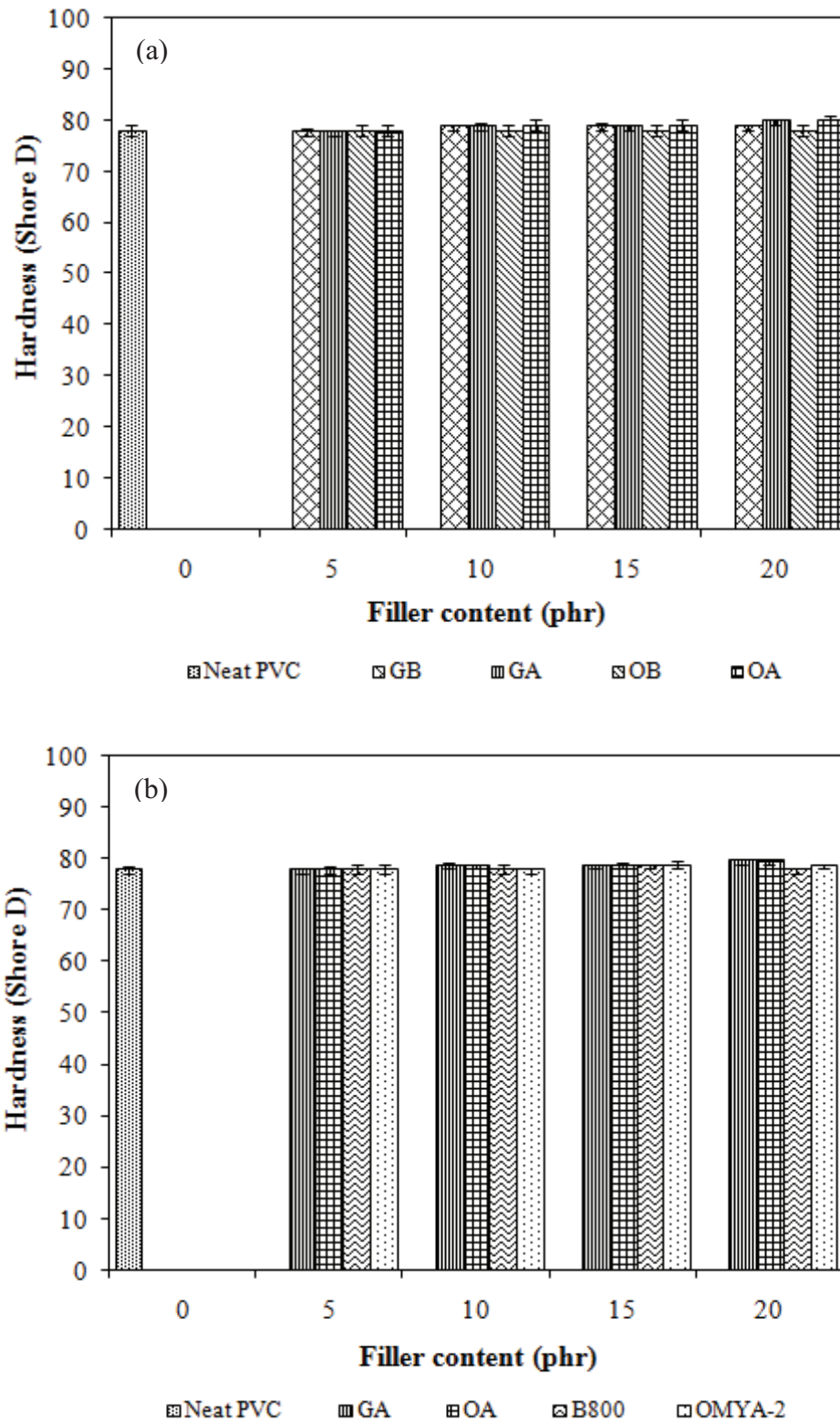
Figure 4.20 Hardness of PVC composites (a) neat PVC, GB, GA, OB
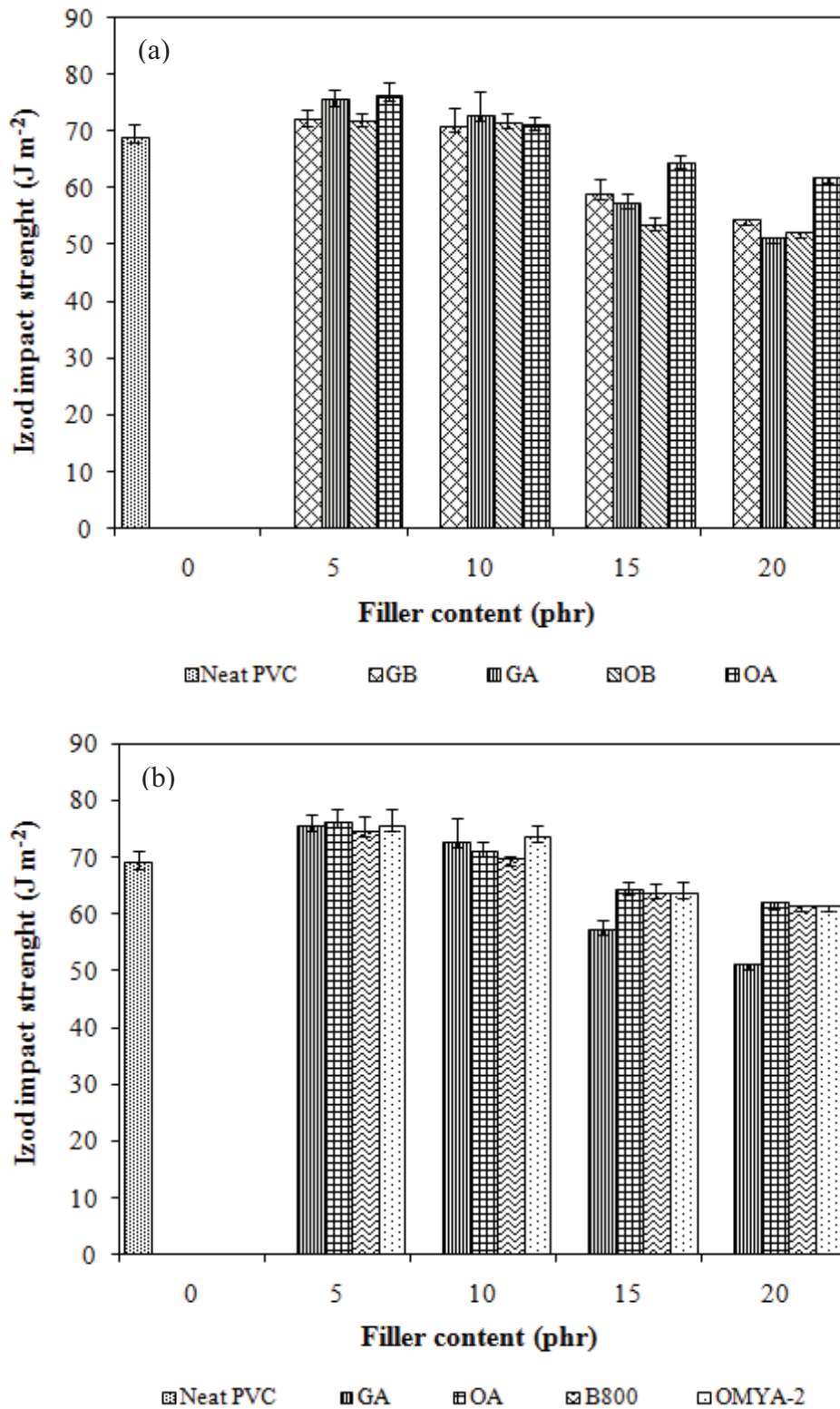and OA, (b) neat PVC, GA, OA, B800 and OMYA-2.

Figure 4.21 Izod impact strength of PVC composites (a) neat PVC, GB, GA, OB and OA, (b) neat PVC, GA, OA, B800 and OMYA-2.

4.6.2 Morphology

Figure 4.22 showed the SEM images of the fracture surface of the PVC composite material by adding 15 phr $CaCO_3$ from golden apple snail and oyster shells before and after hydrothermal process. Figure 4.22(a) and 4.22(b) showed $CaCO_3$ from golden apple snail shells particles and oyster shells particles were not compatible well with PVC matrix due to the large particle size. Additionally, we found the gap between $CaCO_3$ and PVC matrix. However, PVC composite material by adding 15 phr $CaCO_3$ from GA and OA, had a good adhesive interface with PVC matrix, indicating good compatibility of PVC and we could not observe the gap between $CaCO_3$ and PVC matrix in Figure 4.22(c) and 4.22(d). When adding 15 phr $CaCO_3$ from B800, had a good adhesive interface with PVC matrix and by adding 15 phr $CaCO_3$ from OMYA-2 was not compatible well with PVC matrix due to the large particle size in Figure 4.22(e) and 4.22(f). This result confirmed that the smaller particle size of $CaCO_3$ after hydrothermal process, the higher surface area was obtained, resulting the interfacial adhesion between $CaCO_3$ and PVC matrix.

Morphological study of PVC composites revealed that $CaCO_3$ from GA and OA were improved the interfacial adhesion between nano-$CaCO_3$ and PVC matrix. It is well known that the mechanical properties of a particulate filled polymer composite depend on a great extent on good interfacial adhesion, filler dispersion and morphological structure of PVC composites [31-32].
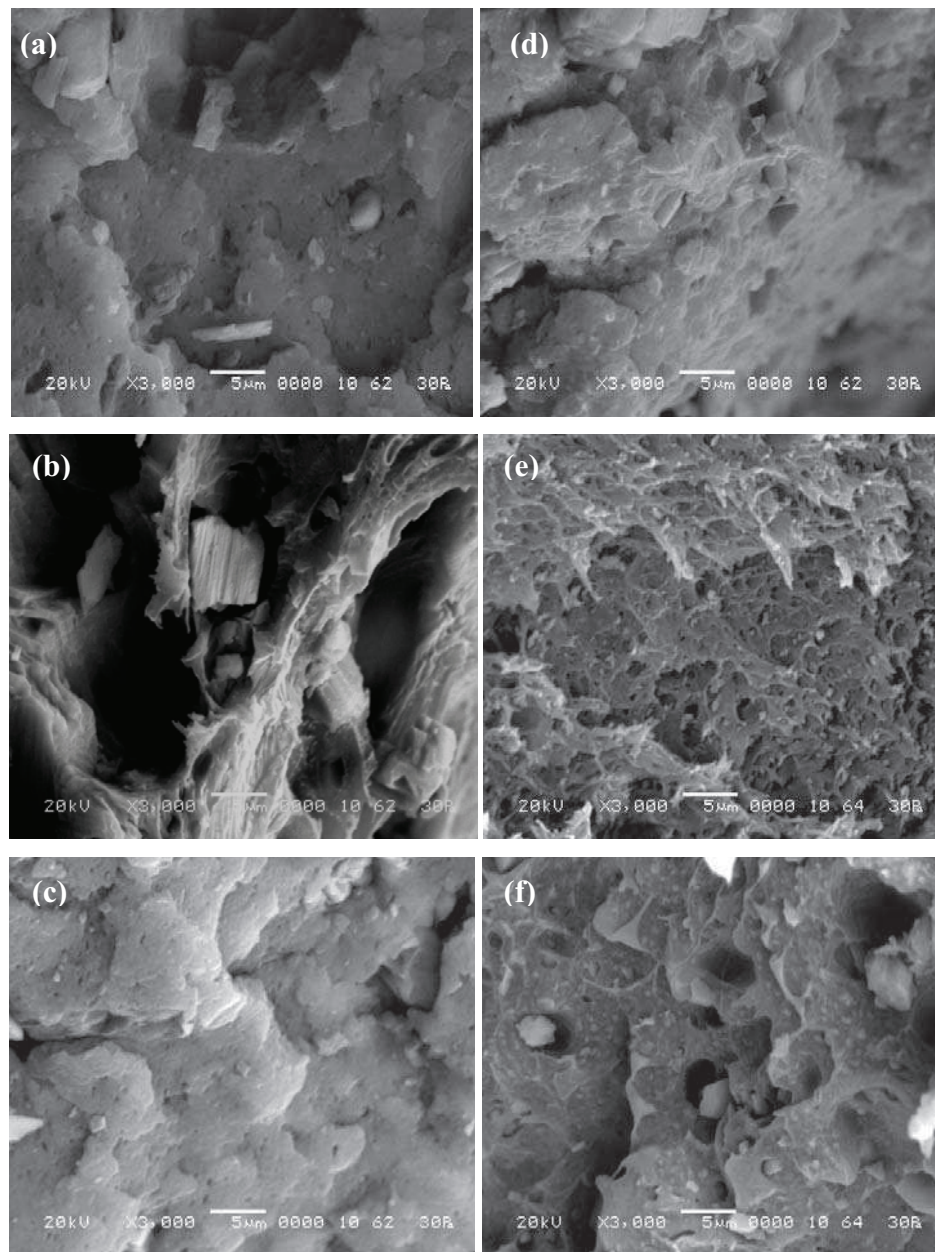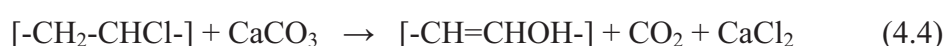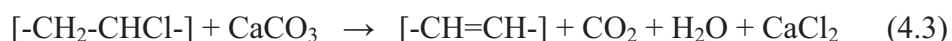
Figure 4.22 Morphology of PVC composites (a) GB, (b) OB, (c) GA,
(d) OA, (e) B800 and (f) OMYA-2.

4.6.3 Thermal Stability

The resulting PVC composite strips were placed in oven at 190±1°C, in order to carry out static thermal stability test by observing the color change of the sample. The thermal stability of PVC is defined by the time taken for the black

decomposition products to appear. The result are illustrated in Figure 4.23. Nest PVC become completely black after 180 min. The result for the PVC composite by adding 15 phr of $CaCO_3$ from GA and OA were improved compared with not only neat PVC but also $CaCO_3$ from golden apple snail shell particles (GB), oyster shells particles (OB) before hydrothermal process filled with PVC. Its stability are better long-term thermal stability than in absence of neat PVC the completely black after 240 min and 270 min.

Nano-$CaCO_3$ from GA and OA are filler often used commercially with PVC resin. The thermal stability is significantly enhanced compared to PVC composite containing nano-$CaCO_3$ commercial (B800) and micro-$CaCO_3$ commercial (OMYA-2) resisting colouring for over 210 min. This indicates that nano-$CaCO_3$ from GA have a pronounced synergetic effect on the stability of PVC [33-34]. Dehydrochlorination of PVC with hydrogen chloride (HCl) elimination creates many problems in PVC processing. Dehydrochlorination of PVC during processing affects only the color, not the other properties. When the mass loss due to dehydrochlorination reaches 0.1%, the color of PVC starts to change. Depending on the number of the conjugated double bonds formed, it becomes yellow, orange, red, brown and black. However, metal soaps are the most used heat stabilizers for PVC [35]. The carboxylate group of the metal salt substitutes the tertiary or allylic chlorine atoms and stops. The above-described behaviors suggested that both $CaCO_3$ took part in reaction of acceptance of HCl without additional influence on kinetic rate of its degradation (except the elimination of HCl catalytic influence) [36]. Both kinds of golden apple snail shells and oyster shells after hydrothermal process showed the higher thermal stability that those golden apple snail shells and oyster shells before hydrothermal process as seen in eq. 4.3 and 4.4.

$$[-CH_2-CHCl-] + CaCO_3 \quad \rightarrow \quad [-CH=CH-] + CO_2 + H_2O + CaCl_2 \quad (4.3)$$

$$[-CH_2-CHCl-] + CaCO_3 \quad \rightarrow \quad [-CH=CHOH-] + CO_2 + CaCl_2 \quad (4.4)$$
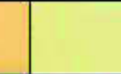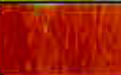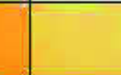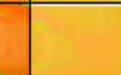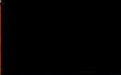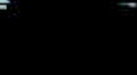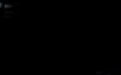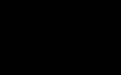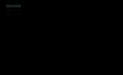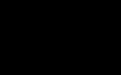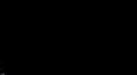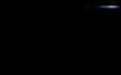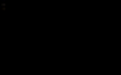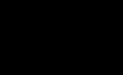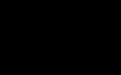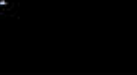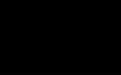
Degradation time	PVC composite material by adding 15 phr of CaCO$_3$						
	Neat PVC	GB	GA	OB	OA	B800	OMYA-2
0							
30							
60							
90							
120							
180							
210							
240							
270							

Figure 4.23 Thermal stability of PVC composite of neat PVC and PVC composite materials by adding 15 phr of GB, GA, OB, OA, B800 and OMYA-2.

4.7   Limiting Oxygen Index of PVC Composite Materials

Figure 4.24 shown the limiting oxygen index (LOI) values of PVC composite materials. The LOI values of neat PVC was 30%O_2. By adding 10 phr of $CaCO_3$ GA, the maximun value of LOI was 34.5%O_2 and by adding 10 phr of $CaCO_3$ OA, the maximun value of LOI was 34.0%O_2. The LOI values of PVC composite material by adding $CaCO_3$ were improved compared with not only neat PVC but also $CaCO_3$ from golden apple snail shell particles (GB), oyster shells particles (OB) before hydrothermal process filled with PVC and commercial $CaCO_3$ (B800 and OMYA-2) filled with PVC. In the presence of heat and oxygen (O_2), PVC composite decomposed to form water vapour, carbon dioxide and HCl, which react with hydrocarbon fragments to produce a very high melting point char at the interface between the polymer and the heat source. The chars rapidly dissipate heat energy and lose their glow. This antiglow property of $CaCO_3$ contributes to its effectiveness as a flame retardant. Accordingly, the LOI values of composite materials seemed to be increased with increasing filler loading and its value of composite material was higher than that of neat PVC when filler was added more than 5 phr. Finally, this is obviously a positive effect because a small amount of nano-$CaCO_3$ is enough to improve the flame resistance of PVC composite materials [37].
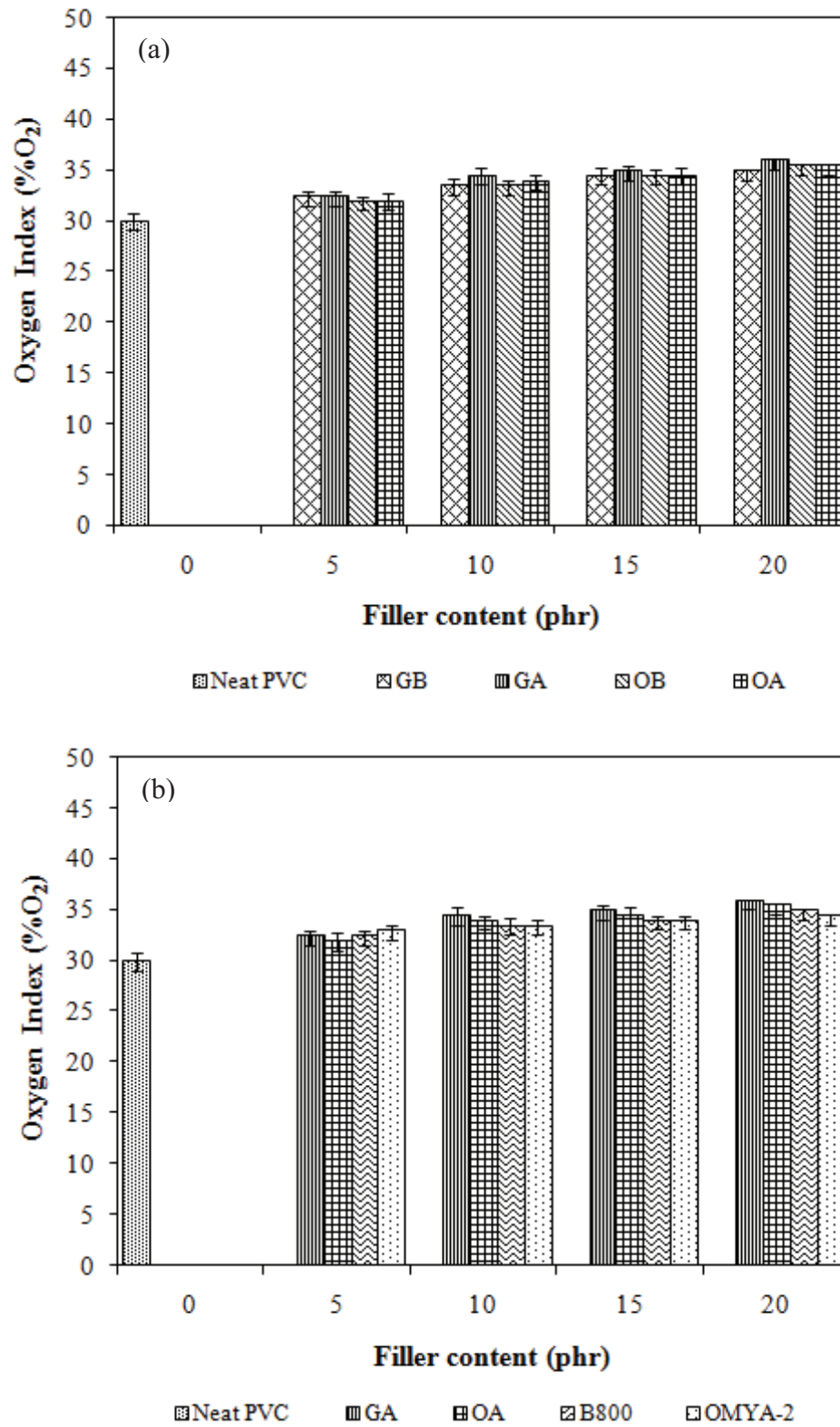
Figure 4.24 Limiting oxygen index values of PVC composites, (a) neat PVC, GB, GA, OB and OA, (b) neat PVC, GA, OA, B800 and OMYA-2.

CHAPTER V

CONCLUSIONS

5.1 Conclusions

In this work, the nano-CaCO$_3$ was synthesized by hydrothermal process. The nano-CaCO$_3$ from golden apple snail shells and oyster shells reinforced PVC composite at various contents (5, 10, 15 and 20 phr) were prepared by using a two-roll mill. The present study could be concluded as follows;

The golden apple snail shells was composed of CaCO$_3$ about 99%, while that of oyster shells was composed of CaCO$_3$ about 97%. The optimum condition for hydrothermal process of producing CaCO$_3$ from golden apple snail shells and oyster shells were obtained at reaction temperature of 100°C for 1 h, the particles size of obtained CaCO$_3$ were in the nano-sized range about 30-850 nm and 74-246 nm.

The tensile strength, elongation at break, hardness, and izod impact strength of the PVC composite material filled with nano-CaCO$_3$ after hydrothermal process were higher than those before hydrothermal process. The morphology study of PVC composites revealed that nano-CaCO$_3$ particles had a good adhesive interface with PVC matrix. The presence of small amounts of nano-CaCO$_3$ increased the thermal stability and LOI value of the PVC composite materials. Finally, the mechanical properties and thermal stability of nano-CaCO$_3$ from golden apple snail or oyster shells after hydrothermal process filled PVC composite materials were similar to those of commercial CaCO$_3$ filled ones.

In this study the nano-CaCO$_3$ from golden apple snail shells or oyster shells after hydrothermal process used as reinforced filler of PVC composites in rigid profile applications. However, the nano-CaCO$_3$ can be used as alternative filler in order to replace of the commercial CaCO$_3$, which is also useful for decreasing the waste products of golden apple snail shells or oyster shells from the environmental issues.

Suggestion for Future Work

In the area of nano-CaCO$_3$ from naturally renewable materials reinforced composite, nano-CaCO$_3$ filler treated with chemical treatment could be used to reinforce the PVC composite at various nano-CaCO$_3$ content of 5, 10, 15, and 20 phr, further study should be done as the following aspects:

1. From the result of this study, the surface of nano-CaCO$_3$ should be treated by adding modification agent to improve the well dispersion in PVC. The nano-CaCO$_3$ should be applied for the commercial production scale of the PVC compound that are used in wire and cable applications.

2. New techniques such as sol gel synthesis or chemical precipitate should be further studied to reduce the high temperature and high pressure of hydrothermal technique.

REFERENCES

[1]   Dunbai, Z., Changgen, C., and Demin, J. Preparation and Mechanical Properties of Solid-phase Grafting Nanocomposites of PVC/Graft Copolymers /MMT. Journal Wuhan University of Technology-Mater. Sci.Ed. 21 (2006) : 4-8.

[2]   Zeng, X.F., Wang, W.Y., Wang, G.Q., and Chen, J.F. Influence of the diameter of $CaCO_3$ particles on the mechanical and rheological properties of PVC composites. Journal Materials science 43 (2008) : 3505-3509.

[3]   Siriprom, W., Kuha, P., and Limsuwan, P. The Computational studies on Molluscan Shells. Procedia Engineering 32 (2012) : 1119-1122.

[4]   Sanico, A.L., Peng, S., Laza, R.C., and Visperas R.M. Effect of seedling age and seedling number per hill on snail damage in irrigated rice. Crop Protection 21 (2002) : 137–143.

[5]   Yoon, G.L., Kim, B.T., Kim B.O., and Han, S.H. Chemical–mechanical characteristics of crushed oyster-shell. Waste Management 23 (2003) : 825–834.

[6]   Odian, G. Principles of polymerization. 4rd ed. New York : John Wiley & Sons, 1991.

[7]   Gachter, R., and Muller, H. Plastics additive handbook. 3rd ed. New York : Hanser, 1990.

[8]   Teo, S.S. Evaluation of different species of fish for biological control of golden apple snail Pomacea canaliculata (Lamarck) in rice. Crop Protection 25 (2006) : 1004-1012.

[9]   Hao, C.T., Shang, L.L., and Jeff, K. Using pretreated waste oyster and clam shells and microwave hydrothermal treatment to recover boron from concentrated waste water. Bioresource Technology 102 (2011) : 7802-7806.

[10]   Katz, H.S., and Milewsht, J.V. Handbook of filler for plastics. 2nd ed. New York : Van nostrand reinhold, 1987.

[11] Feng, B., Yong, A.K., and An, H. Effect of various factors on the particle size of calcium carbonate formed in precipitation process. Materials Science and Engineering A. 445-446 (2007) : 170-179.

[12] Wang, H., Zhang, Q., Yang, H., and Sun, H. Synthesis and microwave dielectric properties of $CaSiO_3$ nanopowder by the sol–gel process. Ceramics International 34 (2008) : 1405-1408.

[13] Byrappa, K., and Adschiri, T. Hydrothermal technology for nanotechnology. Progress in Crystal Growth and Characterization of Materials 53 (2007) : 117-166.

[14] Heiberger, C.A. Encyclopedia of PVC. 2nd ed. New York : Marcell dekker. 1988.

[15] Zhaodong, N., Zuoyi, S., Bianqing, Y., Rong, G., and Wanguo, H. A novel morphology of aragonite and an abnormal polymorph transformation from calcite to aragonite with PAM and CTAB as additives. Journal of Colloid and Interface Science 137 (2008) : 77-182.

[16] Tsuzuki, T., Pethick, K., and McCormick, P.G. Synthesis of $CaCO_3$ nano-particles by mechanochemical processing. Journal Nanoparticle Research 2 (2000) : 375-380.

[17] Montes-Hernandez, G., Fernandez-Martınez, A., Charlet, L., Tisseranda, D., and Renard, F. Textural properties of synthetic nano-calcite produced by hydrothermal carbonation of calcium hydroxide. Journal of Crystal Growth 310 (2008) : 2469-2953.

[18] Udomkan, N., and Limsuwan, N. Temperature effects on freshwater snail shells: *Pomacea canaliculata* Lamarck as investigated by XRD, EDX, SEM and FTIR techniques. Materials Science and Engineering C 28 (2007) : 316-319.

[19] Zeng, X.F., Wang, W.Y., and Wang, G.Q. Influence of the diameter of $CaCO_3$ particles on the mechanical and rheological properties of PVC composites. Journal Materials Science 43 (2008) : 3505–3509.

[20] Hu, H., Dong, P., and Zhen, G. Preparation of active $CaCO_3$ nanoparticles and mechanical properties of the composite materials. Materials Letters 63 (2009) : 373-375.

[21] ASTM Designation : D638-10. Standard test method for tensile properties of plastics.

[22] ASTM Designation : D256-90b. Standrad test methods for impact resistance of plastics and electric insulating material.

[23] Chen, X., and others. Carbonization synthesis of hydrophobic $CaCO_3$ at room temperature. Colloid and Surfaces A: Physicochem. Eng. Aspects 353 (2010) : 97-103.

[24] Gunasekaran, S., and Anbalagan, G. Spectroscopic study of phase transitions in natural calcite mineral. Spectrochimica Acta Past A 69 (2008) : 1246-1251.

[25] Feng, B., Yong, A.K., and An, H. Effect of various factors on the particle size of calcium carbonate formed in a precipitation process. Materials Science and Engineering A 445-446 (2007) : 170-179.

[26] Oganov, A.R., Glass, C.W. and Shigeaki, O. High-pressure phases of $CaCO_3$: Crystal structure prediction and experiment. Earth and Planetary Science Letters 241 (2006) : 95-103.

[27] Pavasupree, S., Ngamsinlapasthian, S., Suzuki, Y., and Yoshikawa, S. Preparation and characterization of high surface area nanosheet titania with mesoporous structure. Materials Letters 61 (2007) : 2973-2977.

[28] Zhaodong, N., Chen, X., Yang, Q., Wang, X., Shi, Z., and Wanguo, H. Structure transition from aragonite to vaterite and calcite by the assistance of SDBS. Journal of Colloid and Interface Science 325 (2008) : 331-336.

[29] Montes-Hernandez, G., Renard, F., Geoffroy, N., Charlet, L., and Pironon, J. Calcite precipitation from CO_2–H_2O–$Ca(OH)_2$ slurry under high pressure of CO. Journal Crystal Growth 308 (2007) : 228-236.

[30] Keiichi, E., and Hiroshi, S. Phase diagram of salt-water system determined by TG-DTA. Thermochimica Acta 327 (1999) : 133-137.

[31] Chen, N., Wan, C., Zhang, Y., and Zhang, Y. Effect of nano-$CaCO_3$ on mechanical properties of PVC and PVC/Blendex blend. Polymer Testing 23 (2004) : 169-174.

[32] Yarahmadi, N., Jakubowicz, I., and Hjertberg, T. The effects of heat treatment and ageing on the mechanical properties of rigid PVC. Polymer Degradation and Stability 82 (2003) : 59-72.

[33] Sterzynski, T., Tomaszewska, J., Piszczek, K., and Skorczewska, K. The influence of carbon nanotubes on the PVC glass transition temperature. Composites Science and Technology 70 (2010) : 966-969.

[34] Lin, Y.J., Li, D.Q., Evans, D.G., and Duan, X. Modulating effect of MgeAleCO₃ layered double hydroxides on the thermal stability of PVC resin. Polymer Degradation and Stability 88 (2005) : 286-293.

[35] Liu, Y.B., Liu, W.Q., and Hou, M.H. Metal dicarboxylates as thermal stabilizers for PVC. Polymer Degradation and Stability 92 (2007) : 1565-1571.

[36] Tongamp, W., Kano, J., Zhang, Q., and Saito, F. Simultaneous treatment of PVC and oyster-shell wastes by mechanochemical means. Waste Management 28 (2008) : 484–488.

[37] La Rosa, A.D., Recca, A., Carter, J.T., and McGrail, P.T. An oxygen index evaluation of flammability on modified epoxy/polyester systems. Polymer 40 (1999) : 4093-4098.

APPENDICES

APPENDIX A

Typical Properties of Commercial CaCO₃

Table A-1   Typical properties of CaCO$_3$ from NPCC-B800

Property	Value
Appearance	White powder
Specific surface, m^2/g	2.5-2.6
Particle size (avg), nm	40
Surface area (BET), m^2/gm	40
Whiteness, %	≥ 90
Particle shape	Cubic
Moisture content, % (wt)	≤ 0.5
CaCO$_3$ % (wt) dry basis	≥ 94.5
MgO % (wt)	≤ 0.6

Table A-2   Typical properties of CaCO$_3$ from OMYACARB-2

Property	Value
Dry whiteness (Ry), (%)	95.220
Fineness pass 325 mesh, (%)	99.998
Mean particle size (d 50 %), (MICRON)	2.880
TOP CUT (d 98 %), (MICRON)	14
Oil absorption, (g paraffin)	36.120
Moisture content, (%)	0.170

APPENDIX B

% Yield of CaCO$_3$ After Hydrothermal Process

Table B-1 % Yield of CaCO$_3$ after hydrothermal process

Sample		Hydrothermal condition			A-HT weight	% Yield
Tybe	Weight	Conc. Na$_2$CO$_3$ (M)	Temp (^{o}C)	Time (h)		
GB	100.0051	2	90	20	84.3490	84.3447
GB	100.1469	1	100	20	72.1370	72.0312
GB	100.0519	2	100	1	86.3289	86.2842
GB	100.5681	2	100	10	85.3556	84.8734
GB	100.7289	2	100	20	86.4718	85.8460
GB	100.6801	3	100	20	90.0641	89.4557
GB	100.0054	2	110	20	84.3970	84.3924
GB	100.0347	2	120	20	84.0035	83.9744
GB	100.0023	2	130	20	87.3278	87.3258
OB	100.0003	2	90	20	83.4490	83.4487
OB	100.1872	1	100	20	73.6652	73.5275
OB	100.0042	2	100	1	85.3600	85.3564
OB	100.0368	2	100	10	84.3590	84.3279
OB	100.0419	2	100	20	85.5120	84.4766
OB	100.5183	3	100	20	89.1096	88.6501
OB	100.0078	2	110	20	83.9467	83.9401
OB	100.0694	2	120	20	84.3679	84.3094
OB	100.0047	2	130	20	86.3200	86.3159

GB, golden apple snail shell particles.
OB, oyster shell particles.
A-HT, after hydrothermall process.

APPENDIX C

Particles Size Distribution of CaCO$_3$ from Golden Apple Snail Shells and Oyster Shells Before and After Hydrothermal Process
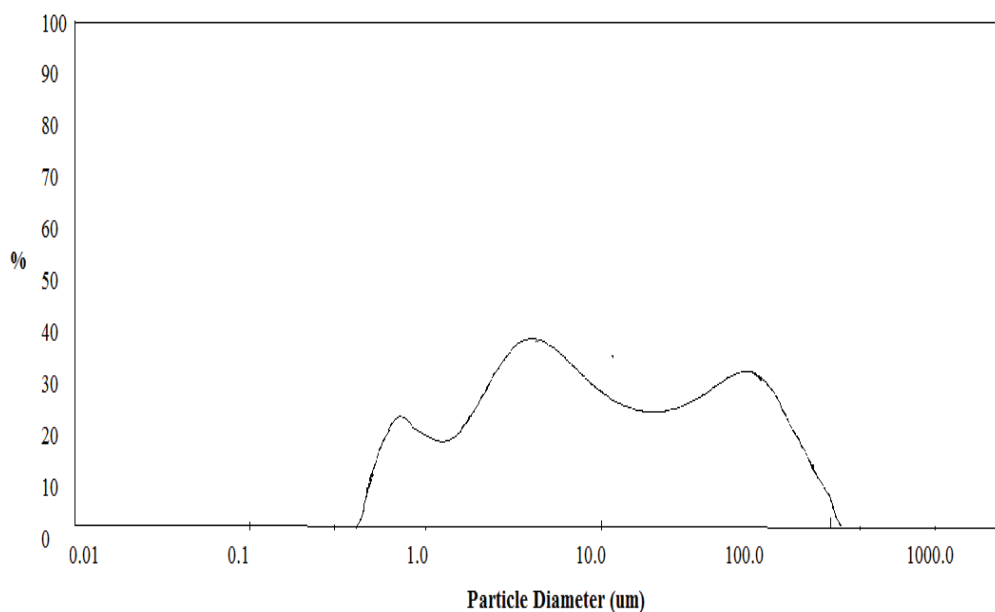
Figure C-1 Particles size distribution of CaCO$_3$ from golden apple snail shell particles.
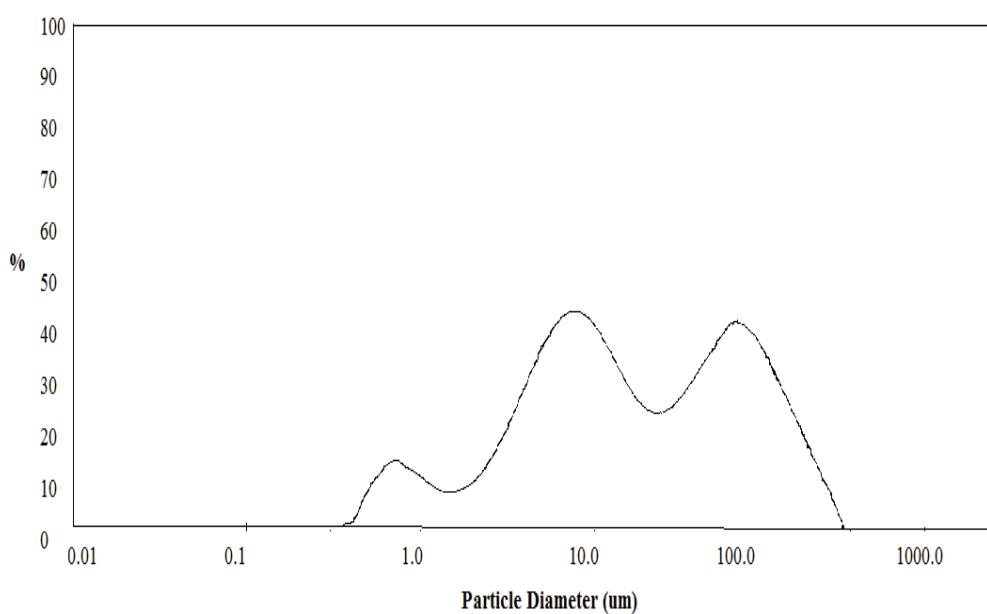
Figure C-2 Particles size distribution of CaCO$_3$ from oyster shell particles.
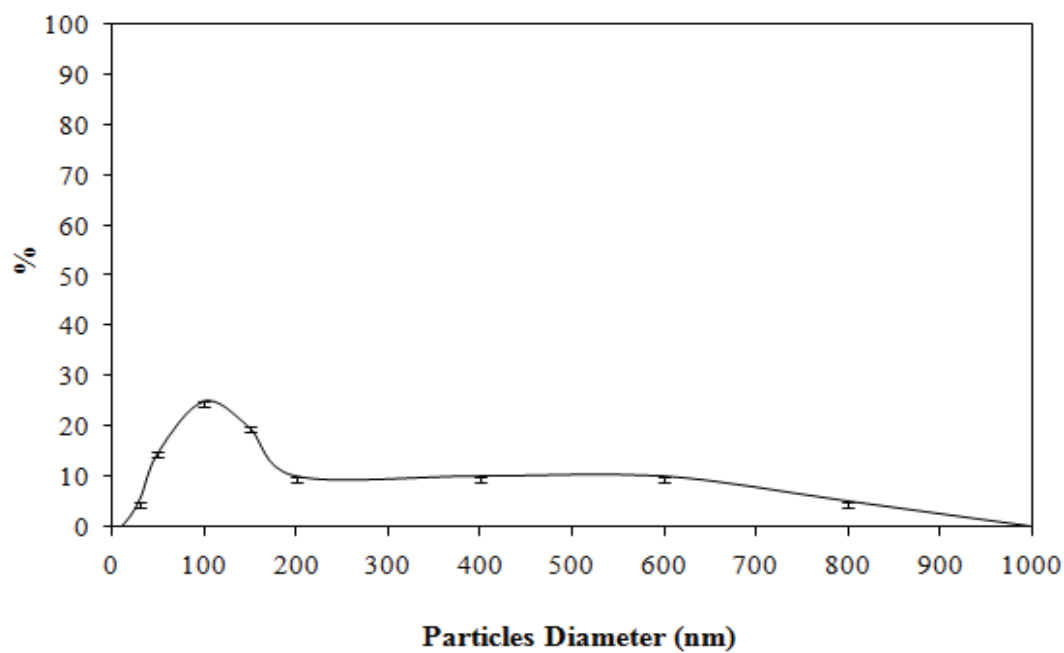
Figure C-3 Particles size distribution of CaCO$_3$ from golden apple snail shell particles under the optimum condition of hydrothermal process at 100°C for 1 h, Na$_2$CO$_3$ 2 M.
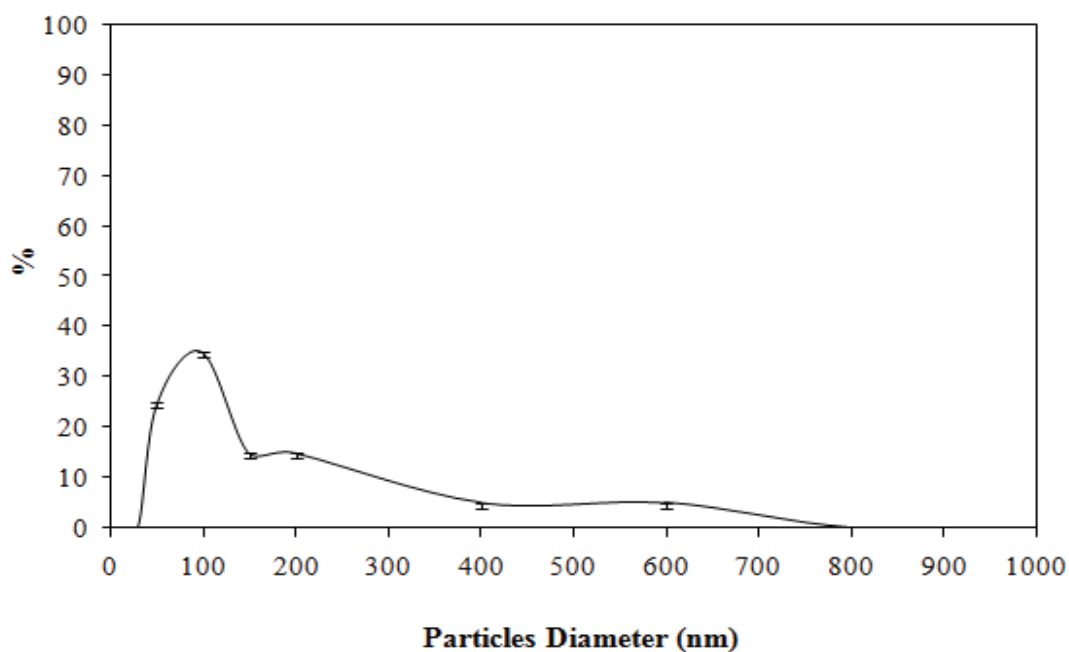
Figure C-4 Particles size distribution of CaCO$_3$ from oyster shell particles under the optimum condition of hydrothermal process at 100°C for 1 h, Na$_2$CO$_3$ 2 M.

APPENDIX D

Mechanical Properties and Thermal stability of Composites

Table D-1   Tensile strength of PVC composites

Sample	No.	Tensile strength (Mpa) in each filler content (phr)				
		0	5	10	15	20
neat PVC	1	31.9	-	-	-	-
	2	31.2	-	-	-	-
	3	30.4	-	-	-	-
	4	30.8	-	-	-	-
	5	31.4	-	-	-	-
	mean	31.1	-	-	-	-
	SD	0.6	-	-	-	-
	3SD	1.2	-	-	-	-
GB	1	-	30.0	29.4	28.1	28.9
	2	-	32.7	32.8	27.9	26.1
	3	-	33.1	28.7	28.5	25.3
	4	-	30.5	30.6	28.0	28.5
	5	-	30.2	30.1	27.4	27.9
	mean	-	31.3	30.3	28.0	27.3
	SD	-	1.5	1.6	0.4	1.6
	3SD	-	4.5	4.8	1.2	4.8
OB	1	-	30.9	31.1	31.8	29.4
	2	-	30.7	30.5	29.2	29.8
	3	-	31.2	31.6	27.6	27.4
	4	-	32.7	28.8	32.1	27.1
	5	-	30.1	31.7	27.5	28.3
	mean	-	31.1	30.7	29.6	28.4
	SD	-	1.0	1.2	2.2	1.2
	3SD	-	3.0	3.6	6.6	3.6
GA	1	-	36.9	34.6	33.4	30.9
	2	-	35.8	35.7	33.8	30.3
	3	-	35.6	32.2	31.7	32.7
	4	-	36.9	34.8	34.0	29.9
	5	-	36.2	34.1	33.9	32.6
	mean	-	36.3	34.3	33.4	31.3
	SD	-	0.6	1.3	1.0	1.3
	3SD	-	1.8	3.9	3.0	3.9
OA	1	-	36.7	33.3	31.9	32.6
	2	-	37.4	33.7	32.1	30.9
	3	-	35.1	33.4	31.8	32.8
	4	-	38.2	34.8	33.6	29.8
	5	-	36.1	34.1	31.6	30.5
	mean	-	36.7	33.9	32.2	31.3
	SD	-	1.2	0.6	0.8	1.3
	3SD	-	3.6	1.8	2.4	3.6
B800	1	-	38.2	35.6	32.6	33.3
	2	-	37.1	33.0	32.6	33.0
	3	-	36.5	35.7	34.1	32.4
	4	-	36.7	34,8	34.7	31.5
	5	-	35.3	33.9	32.9	33.3
	mean	-	36.8	34.6	33.4	32.7
	SD	-	1.0	1.3	1.0	0.8
	3SD	-	3.9	3.9	3.0	2.4
OMYA2	1	-	36.9	35.4	33.1	32.2
	2	-	37.0	36.2	33.9	34.3
	3	-	37.4	33.3	34.9	31.2
	4	-	36.1	35.1	32.4	32.5
	5	-	36.3	35.8	32.1	32.4
	mean	-	36.7	35.2	33.3	32.5
	SD	-	0.5	1.1	1.1	1.1
	3SD	-	1.5	3.3	3.3	3.3

Table D-2   Elongation at break of PVC composites

Sample	No.	Elongation at break (%) in each filler content (phr)				
		0	5	10	15	20
neat PVC	1	158.1	-	-	-	-
	2	179.1	-	-	-	-
	3	164.1	-	-	-	-
	4	170.3	-	-	-	-
	5	159.2	-	-	-	-
	mean	166.2	-	-	-	-
	SD	8.7	-	-	-	-
	3SD	26.1	-	-	-	-
GB	1	-	185.2	188.8	131.9	111.9
	2	-	204.8	157.7	176.8	128.2
	3	-	152.4	180.6	175.9	121.7
	4	-	168.9	166.7	145.7	136.3
	5	-	170.4	159.4	160.3	129.2
	mean	-	176.3	170.6	158.1	125.5
	SD	-	19.7	13.6	19.4	9.2
	3SD	-	59.1	40.8	58.2	27.6
OB	1	-	202.9	189.6	122.9	125.8
	2	-	200.8	179.9	141.8	123.4
	3	-	186.1	172.0	179.6	145.0
	4	-	195.7	174.6	172.4	129.4
	5	-	185.1	168.9	133.4	127.3
	mean	-	194.1	177.0	150.0	130.2
	SD	-	8.2	8.1	24.8	8.6
	3SD	-	24.6	24.3	74.4	25.8
GA	1	-	197.7	175.9	171.3	155.5
	2	-	194.6	179.3	174.3	142.0
	3	-	194.6	187.0	145.9	153.7
	4	-	200.7	190.2	168.3	139.4
	5	-	203.1	170.2	167.9	136.6
	mean	-	198.1	180.5	165.5	145.4
	SD	-	3.8	8.1	11.3	8.6
	3SD	-	11.4	24.3	33.9	25.8
OA	1	-	201.5	183.8	147.2	128.9
	2	-	203.2	185.1	178.8	136.1
	3	-	196.6	184.2	156.9	115.2
	4	-	170.0	163.6	167.7	127.2
	5	-	195.4	183.8	155.0	138.8
	mean	-	193.3	180.1	161.1	129.2
	SD	-	13.4	9.2	12.3	9.2
	3SD	-	40.3	27.6	36.9	27.6
B800	1	-	202.2	192.9	163.9	177.0
	2	-	201.6	181.6	185.4	185.4
	3	-	205.2	176.6	173.8	172.3
	4	-	201.3	179.3	188.4	161.9
	5	-	200.7	184.2	174.0	167.3
	mean	-	202.2	182.9	177.1	172.8
	SD	-	1.8	6.3	9.9	9.0
	3SD	-	5.4	18.9	29.7	24.0
OMYA2	1	-	202.6	193.5	163.5	165.3
	2	-	204.1	204.3	138.1	163.2
	3	-	203.2	206.3	173.1	152.8
	4	-	199.3	199.2	157.3	147.2
	5	-	200.8	201.5	164.9	164.0
	mean	-	202.0	201.0	159.4	158.5
	SD	-	1.9	5.0	13.2	8.0
	3SD	-	5.7	25.0	39.6	24.0

Table D-3   Hardness of PVC composites

Sample	No.	Hardness (Shore D) in each filler content (phr)				
		0	5	10	15	20
neat PVC	1	78.0	-	-	-	-
	2	78.0	-	-	-	-
	3	77.5	-	-	-	-
	4	78.5	-	-	-	-
	5	78.0	-	-	-	-
	mean	78.0	-	-	-	-
	SD	0.4	-	-	-	-
	3SD	1.2	-	-	-	-
GB	1	-	78.0	79.0	79.0	79.0
	2	-	78.0	78.5	79.0	79.0
	3	-	78.0	79.0	79.0	79.5
	4	-	78.0	79.0	79.0	78.5
	5	-	78.0	79.5	79.0	79.0
	mean	-	78.0	79.0	79.0	79.0
	SD	-	0.0	0.4	0.0	0.4
	3SD	-	0.0	1.2	0.0	1.2
OB	1	-	78.0	78.0	78.0	78.0
	2	-	78.0	79.0	78.0	78.0
	3	-	78.0	78.0	78.0	78.0
	4	-	78.0	78.0	78.0	78.0
	5	-	78.0	77.0	78.0	78.0
	mean	-	78.0	78.0	78.0	78.0
	SD	-	0.0	0.7	0.0	0.0
	3SD	-	0.0	2.1	0.0	0.0
GA	1	-	78.0	79.0	79.0	80.0
	2	-	78.0	79.0	78.5	80.0
	3	-	78.0	79.0	79.0	80.0
	4	-	78.0	79.0	79.0	80.0
	5	-	78.0	79.0	79.5	80.0
	mean	-	78.0	79.0	79.0	80.0
	SD	-	0.0	0.0	0.4	0.0
	3SD	-	0.0	0.0	1.2	0.0
OA	1	-	78.0	79.0	79.0	80.0
	2	-	78.0	78.5	79.0	80.0
	3	-	78.0	79.5	79.0	80.0
	4	-	78.0	79.0	79.0	79.5
	5	-	78.0	79.0	79.0	80.5
	mean	-	78.0	79.0	79.0	80.0
	SD	-	0.0	0.4	0.0	0.4
	3SD	-	0.0	1.2	0.0	1.2
B800	1	-	78.0	78.0	79.0	80.0
	2	-	79.0	78.0	79.0	80.0
	3	-	78.0	79.0	80.0	80.0
	4	-	78.0	77.0	79.0	80.0
	5	-	77.0	78.0	78.0	80.0
	mean	-	78.0	78.0	79.0	80.0
	SD	-	0.7	0.7	0.7	0.0
	3SD	-	2.1	2.1	2.1	0.0
OMYA2	1	-	78.0	78.0	79.0	80.0
	2	-	78.0	79.0	79.0	81.0
	3	-	78.5	78.0	79.0	80.0
	4	-	77.5	77.0	79.0	79.0
	5	-	78.0	78.0	79.0	80.0
	mean	-	78.0	78.0	79.0	80.0
	SD	-	0.4	0.7	0.0	0.7
	3SD	-	1.2	2.1	0.0	2.1

Table D-4   Izod impact strenght of PVC composites

Sample	No.	Izod impact strenght ($J\ m^{-2}$) in each filler content (phr)				
		0	5	10	15	20
neat PVC	1	67.01	-	-	-	-
	2	70.41	-	-	-	-
	3	67.78	-	-	-	-
	4	71.92	-	-	-	-
	5	68.00	-	-	-	-
	mean	69.02	-	-	-	-
	SD	2.06	-	-	-	-
	3SD	6.18	-	-	-	-
GB	1	-	70.71	70.61	59.55	53.15
	2	-	71.01	68.54	53.47	51.90
	3	-	72.56	69.32	59.37	57.78
	4	-	73.37	72.58	62.40	53.18
	5	-	72.31	72.78	60.11	56.72
	mean	-	71.99	70.77	58.98	54.55
	SD	-	1.11	1.90	3.31	2.55
	3SD	-	3.33	5.70	9.93	7.65
OB	1	-	70.15	73.64	53.46	53.14
	2	-	73.41	70.25	55.61	51.09
	3	-	72.59	71.44	54.75	52.74
	4	-	71.26	71.00	51.06	51.29
	5	-	71.13	70.81	53.19	53.46
	mean	-	71.71	71.43	53.61	52.34
	SD	-	1.29	1.31	1.73	1.09
	3SD	-	3.87	3.93	5.19	3.27
GA	1	-	76.20	74.51	50.11	50.16
	2	-	76.13	72.08	59.83	49.31
	3	-	75.30	74.49	59.00	53.66
	4	-	74.71	70.00	58.19	51.95
	5	-	75.29	72.63	59.46	51.08
	mean	-	75.53	72.74	57.32	51.23
	SD	-	0.63	1.88	4.08	1.68
	3SD	-	1.89	5.64	12.24	5.04
OA	1	-	76.00	73.00	64.12	62.41
	2	-	76.89	73.67	65.59	60.15
	3	-	78.01	70.21	66.01	63.79
	4	-	74.75	68.20	62.57	62.00
	5	-	76.03	71.13	64.12	61.59
	mean	-	76.34	71.24	64.48	61.99
	SD	-	1.21	2.20	1.37	1.32
	3SD	-	3.63	6.60	4.11	3.96
B800	1	-	73.31	67.93	63.79	63.01
	2	-	72.67	70.90	62.73	59.46
	3	-	77.38	73.78	64.00	60.24
	4	-	75.98	67.20	63.58	61.80
	5	-	74.00	68.55	64.21	63.44
	mean	-	74.67	69.67	63.66	61.59
	SD	-	1.96	2.68	0.57	1.72
	3SD	-	5.88	8.04	1.71	5.16
OMYA2	1	-	77.20	71.13	62.79	63.01
	2	-	78.31	73.44	63.15	63.79
	3	-	73.73	71.26	65.70	59.14
	4	-	74.02	76.25	61.64	60.25
	5	-	75.33	77.01	65.22	61.39
	mean	-	75.72	73.82	63.70	61.52
	SD	-	1.99	2.74	1.71	1.91
	3SD	-	5.97	8.22	5.13	5.73

Table D-5 Limiting oxyen index of PVC composites

Sample	No.	Limiting oxyen index (%O_2) in each filler content (phr)				
		0	5	10	15	20
neat PVC	1	30.0	-	-	-	-
	2	31.0	-	-	-	-
	3	30.0	-	-	-	-
	4	29.0	-	-	-	-
	5	30.0	-	-	-	-
	mean	30.0	-	-	-	-
	SD	0.7	-	-	-	-
	3SD	2.1	-	-	-	-
GB	1	-	32.5	33.5	34.5	35.0
	2	-	32.0	33.5	33.0	35.0
	3	-	32.5	34.0	34.0	34.0
	4	-	33.0	33.5	34.5	36.0
	5	-	32.5	33.0	34.5	35.0
	mean	-	32.5	33.5	34.1	35.0
	SD	-	0.4	0.4	0.7	0.7
	3SD	-	1.2	1.2	2.1	2.1
OB	1	-	32.0	33.5	34.5	35.5
	2	-	33.0	33.0	34.5	35.0
	3	-	32.0	34.0	34.5	35.0
	4	-	32.0	33.5	35.0	36.0
	5	-	31.0	33.5	34.0	36.0
	mean	-	32.0	33.5	34.5	35.5
	SD	-	0.7	0.4	0.4	0.5
	3SD	-	2.1	1.2	1.2	1.5
GA	1	-	32.5	34.5	35.0	35.5
	2	-	32.5	35.0	35.0	35.0
	3	-	32.5	34.0	36.0	36.0
	4	-	33.0	34.5	34.0	35.5
	5	-	32.0	34.5	35.0	35.5
	mean	-	32.5	34.5	35.0	35.5
	SD	-	0.4	0.4	0.7	0.4
	3SD	-	1.2	1.2	2.1	1.2
OA	1	-	32.0	34.0	34.5	36.0
	2	-	31.0	33.0	34.0	35.0
	3	-	32.0	35.0	35.0	36.0
	4	-	33.0	34.0	34.5	37.0
	5	-	32.0	34.0	34.5	36.0
	mean	-	32.0	34.0	34.5	36.0
	SD	-	0.7	0.7	0.4	0.7
	3SD	-	2.1	2.1	1.2	2.1
B800	1	-	32.5	33.5	34.0	35.0
	2	-	32.0	33.5	34.0	35.0
	3	-	33.0	33.0	34.0	35.0
	4	-	32.5	34.0	35.0	34.5
	5	-	32.5	33.5	33.0	35.5
	mean	-	32.5	33.5	34.0	35.0
	SD	-	0.4	0.4	0.7	0.4
	3SD	-	1.2	1.2	2.1	1.2
OMYA2	1	-	33.0	33.5	34.0	34.5
	2	-	33.0	33.0	34.0	34.0
	3	-	34.0	34.0	34.5	35.0
	4	-	32.0	33.5	33.5	34.5
	5	-	33.0	33.5	34.0	34.5
	mean	-	33.0	33.5	34.0	34.5
	SD	-	0.7	0.4	0.4	0.4
	3SD	-	2.1	1.2	1.2	1.2

VITA

Ms. Nittima Rungpin was born on February 25, 1983 at Mae Rim District, Chiangmai Province. She received her Bachelor's Degree of Science (Chemistry) in Chemistry Department at the Faculty of Science, Maejo University in 2006. She began her Master study in Program of Petrochemistry and Polymer Science, Faculty of Science, Chulalongkorn University in November 2009 and completed the program in May 2012.

Presentation: "Preparation of calcium carbonate from Thai golden apple snail shells by hydrothermal process as reinforcing filler for poly(vinyl chloride)" proceedings of PACCON 2011, Bangkok, Thailand, January 5 - 7, 2011.